# *Tet*(C) gene transfer between *Chlamydia suis* strains occurs by homologous recombination after co-infection: Implications for spread of tetracycline-resistance among *Chlamydiaceae*

Hanna Marti[a*], Hoyon Kim[a], Sandeep J. Joseph[b,c], Stacey Dojiri[a], Timothy D. Read[b,c], Deborah Dean[a,d]#

Center for Immunobiology and Vaccine Development, UCSF Benioff Children's Hospital Oakland Research Institute, Oakland, California, USA[a]; Department of Medicine, Division of Infectious Diseases[b] and Department of Human Genetics, Emory University School of Medicine, Atlanta, Georgia, USA[c]; Joint Graduate Program in Bioengineering, University of California, San Francisco, California, USA, and University of California, Berkeley, Berkeley, California, USA[d].

Running title: *C. suis tet*(C) transfer model

*Present address: Institute of Veterinary Pathology, Vetsuisse Faculty, University of Zurich, Switzerland

TDR and DD contributed equally to this work

#Address corresponding to Deborah Dean, ddean@chori.org



PeerJ Preprints | https://doi.org/10.7287/peerj.preprints.2489v1 | CC BY 4.0 Open Access | rec: 30 Sep 2016, publ: 30 Sep 2016

**Abstract**

*Chlamydia suis* is a swine pathogen that also causes zoonotic infections. Many strains contain a *tet*(C) cassette conferring tetracycline resistance originally acquired by horizontal gene transfer from a Gram-negative donor. As we and others have described the capacity for *Chlamydiaceae* to exchange DNA by homologous recombination, *tet*(C)-containing *C. suis* strains represent a potential source for antibiotic-resistance spread within and between *Chlamydia* species. Here, we examine the genetics of *tet*(C)-transfer among *C. suis* strains. Tetracycline-sensitive *C. suis* strain S45 was simultaneously or sequentially co-infected with tetracycline-resistant *C. suis* strains in McCoy cells. Potential recombinants were clonally purified by plaque assay. *C. suis* strain Rogers132, which lacks IS*200*/IS*605* transposases, was the most efficient donor, producing three confirmed recombinants of 56 (5.4%) clones with a minimal inhibitory concentration (MIC) of ~8µg/mL. Resistance was stable when recombinants were grown initially in tetracycline at twice the MIC of S45 (0.032 µg/mL). Genomic analysis revealed that *tet*(C) had integrated into the S45 genome by homologous recombination at two sites in different recombinants: a 55kb exchange between *nrq*F and *pckG*, and a 175kb exchange between *kds*A and *cys*Q. Neither site was associated with repeats or motifs associated with recombination hotspots. Our findings show that cassette transfer into S45 has low frequency, does not require IS*200*/IS*605* transposases, is stable if initially grown in tetracycline, and results in multiple genomic configurations. We provide a model for stable cassette transfer to better understand the capability for cassette acquisition by *Chlamydia* species that infect humans, a matter of public health importance.

## INTRODUCTION

Bacteria develop resistance to antibiotics either as a result of mutation in their chromosomal genes or from acquisition of antibiotic resistance transposons by horizontal gene transfer (HGT). Reports of bacterial resistance to antimicrobial agents have occurred almost simultaneously with their first introduction in the late 1930s (1). Resistance through mutation or HGT is promoted by high doses of antibiotics; the use of sub-inhibitory concentrations and broad-spectrum antibiotics; patient non-compliance with the treatment regimens; and the use of antibiotics in lower mammalian and avian species that are bred for human consumption (2). These latter practices have led to an alarming increase in microbial pathogen resistance such as colistin-resistant *Escherichia coli* and multidrug-resistant *Staphylococcus aureus*. Both have been isolated from pigs and zoonotically transmitted to human hosts (3, 4), adding to the current crisis in public health infectious disease control (5, 6).

While there are five families of obligate intracellular bacteria that infect mammals, including *Ehrlichiaceae*, *Anaplasmataceae*, *Rickettsiaceae*, *Coxiellaceae* and *Chlamydia*, *Chlamydia suis* is the only reported obligate intracellular bacterium to have naturally acquired the tetracycline resistance gene *tet*(C), which occurred by HGT (7, 8). This organism is a pig pathogen associated with conjunctivitis, pneumonia, diarrhea/enteritis and reproductive disorders in addition to unapparent infection (9, 10). *C. suis* has also recently been associated with zoonoses including trachoma (a chronic ocular disease) (11), ocular infection in abattoir workers (12) and asymptomatic nasal, pharyngeal and intestinal infections in farmers (13).

Tetracyclines, including doxycycline, are used to treat a wide variety of bacteria including all species of *Chlamydia*, in particular, complicated infections caused by the human pathogen *Chlamydia trachomatis* (14). Since both *C. suis* and *C. trachomatis* infect the human



PeerJ Preprints | https://doi.org/10.7287/peerj.preprints.2489v1 | CC BY 4.0 Open Access | rec: 30 Sep 2016, publ: 30 Sep 2016

conjunctiva and rectum, the *in vivo* opportunity for HGT of the *tet*(C) cassette to *C. trachomatis* is a real concern. Indeed, *C. suis and C. trachomatis* co-infections have been reported among trachoma patients (11).

Tetracycline resistance in *C. suis* is conferred by a variable cassette containing the tetracycline class C gene [*tet*(C)], which encodes an efflux pump to export tetracycline from infected cells. Three *tet*(C) cassettes have been identified and described among *C. suis* strains (7, 15). One is comprised of *tet*(C), the tetracycline repressor gene *tet*R(C), replication genes *rep*AC as well as mobilization genes *mob*ABCDE and two insertion sequences, IS*605* and IS*200* that contain transposases. Another cassette possesses *tet*(C) and *tet*R(C) as well as the two transposases but lacks the replication and mobilization genes. A third cassette is missing only the IS*200*/IS*605* transposases. Dugan *et al.* (16) used an *Escherichia coli*-based mating assay to show that the IS*605* transposases are most likely responsible for the integration of the cassette into the *C. suis* genome. In further analyses, Suchland *et al*. (17) was able to develop a co-infection model and successfully generate tetracycline resistant ($tet^R$) *C. trachomatis* $L_2$ strains from co-infection with *C. suis* R19, which contains both transposases, and a tetracycline sensitive ($tet^S$) $L_2$ strain. However, cassettes lacking the transposases have not been studied for their recombinogenic potential. Here, we tested the requirement of IS*200*/IS*605* transposases for *tet*(C)-containing cassette transfer and developed a model system to study cassette transfer among chlamydiae in the presence and absence of tetracycline.



PeerJ Preprints | https://doi.org/10.7287/peerj.preprints.2489v1 | CC BY 4.0 Open Access | rec: 30 Sep 2016, publ: 30 Sep 2016

## MATERIALS AND METHODS

***Chlamydia* strains, tissue culture and tetracycline susceptibility.** Table 1 describes the strains used in this study. All strains were individually propagated in McCoy cells prior to density gradient purification as previously described (15, 18). McCoy cells were screened for *Mycoplasma* contamination before use (Universal Mycoplasma Detection Kit, ATCC® 30-1012K™ Manassas, Virginia). Briefly, McCoy cells were grown in medium consisting of 450 mL Minimal Essential Medium alpha (MEMa, Life technologies, Carlsbad, CA), 10% Fetal Bovine Serum (FBS, JR Scientific, Woodland, CA), 15 mL sodium bicarbonate (2.8%) (Thermo Fisher Scientific, Waltham, MA), 10 mL glucose (45%) (Fisher Scientific), 10 mM HEPES (Life technologies), 100 µg/mL Vancomycin (Fisher Scientific) and 40µg/mL Gentamycin (Fisher Scientific). All infections were grown in propagation medium consisting of growth medium supplemented with 1.4 µg/mL Cycloheximide (Sigma Aldrich, St. Louis, MO) as well as NGV-Amp B solution (29 U/mL Nystatin, 11.85 µg/mL Gentamycin, 29.62 µg/mL Vancomycin and 2.22 µg/mL Amphoteracin B (Sigma Aldrich)) at 37°C in 5% $CO_2$.

The *in vitro* tetracycline susceptibility was determined as the minimal inhibitory concentrations (MIC) according to Suchland *et al.* (19) with minor changes. Briefly, each chlamydial strain was inoculated onto 20 wells of a 48-well plate (E & K Scientific, Santa Clara, CA) seeded with McCoy cells at a multiplicity of infection (MOI) of 0.5 or 1 depending on the infectivity of the strain. Two wells served as negative controls and were inoculated with 100 µL propagation medium. After inoculation of cells, the plate was centrifuged at 1500 RPM for 1 h at 37 °C. A tetracycline (Sigma-Aldrich) stock solution was prepared at a concentration of 10 mg/mL in dd$H_2O$, and used for a twofold dilution in propagation medium without antibiotics with final concentrations ranging of 0.002 to 256 µg/mL (18 concentrations). After



PeerJ Preprints | https://doi.org/10.7287/peerj.preprints.2489v1 | CC BY 4.0 Open Access | rec: 30 Sep 2016, publ: 30 Sep 2016

centrifugation, the chlamydial inocula were aspirated and replaced with the serial tetracycline dilutions. Two infected and two uninfected wells received propagation medium without any tetracycline and served as positive and negative controls, respectively. After 24 to 36 hours, depending on the developmental cycle of the strain, medium was removed and cells were washed three times with PBS (Gibco, Fisher Scientific) before they were fixed with methanol (-20°C) for 10 min. Chlamydial inclusions were detected by direct immunofluorescence using *Chlamydia* Confirmation Pathfinder (Bio-Rad, Hercules, CA) or FITC conjugated anti-chlamydial LPS monoclonal antibody (ProSci, Poway, CA) at a 1:15 dilution. The MICs of the strains were evaluated by analyzing size and morphology as well as the number of inclusions at 200 X using a Nikon Eclipse Microscope and SPOT imaging software (Diagnostic Instruments, Inc. Sterling Heights, MI). As defined by Suchland et al. (17), we determined the MIC transition point ($MIC_{TP}$) to be the tetracycline concentrations where 90% or more of the inclusions displayed alterations in size and morphology. Furthermore, twofold higher concentrations (two times the $MIC_{TP}$) were considered to be the actual MIC.

**Generation and clonal isolation of recombinants.** Two different recombination protocols were applied in regards to co-infection. For Protocol 1 (recipient-first co-infection), $tet^S$ S45 at a multiplicity of infection (MOI) of 4 was used to infect 80-100% confluent McCoy cell monolayers in shell vials (E & K) (without centrifugation) and incubation at 37 °C for 24 hrs before the addition of $tet^R$ Rogers132, $tet^R$ R19, or $tet^R$ R27 (MOI 0.5). Tetracycline challenge was at 2 µg/mL (1/2 $MIC_{TP}$ Rogers132) as described below. For protocol 2 (simultaneous co-infection), $tet^S$ S45 was first grown in McCoy cell monolayers in shell vials to reach 100% infection; 25-50µL of the infected culture were transferred to a new shell vial with a 80-100%



PeerJ Preprints | https://doi.org/10.7287/peerj.preprints.2489v1 | CC BY 4.0 Open Access | rec: 30 Sep 2016, publ: 30 Sep 2016

confluent McCoy cell monolayer and simultaneously or consecutively co-infected with $tet^R$ R19 or $tet^R$ Rogers132 8 to 24 hours post infection (pi) with $tet^S$ S45. Centrifugation was then performed for 1h at 1500 RPM. Tetracycline challenge was with 0.25 µg/mL (8x MIC S45) as described below (Fig. S1).

For each co-infection, three conditions and two controls (single infection with each parental strain) were used. All co-infection experiments were performed in glass shell vials with one shell vial per condition. Condition A did not contain any tetracycline (no tet); Condition B contained sub-inhibitory concentrations of tetracycline (1/2 $MIC_{TP}$ for S45; 0.004 µg/mL); and Condition C contained two times the MIC of S45 (0.032 µg/mL). Co-infected cultures were propagated for 72 hours, sonicated once (20% amplitude, Sonic Dismembrator Ultrasonic Processor, Fisher Scientific), and new shell vials were infected to produce 100% infection. Each condition was either directly challenged with tetracycline (2 or 0.25 µg/mL depending on protocol one or two described above) or passaged once in propagation medium without antibiotics prior to the tetracycline challenge. Following the challenge for 36 to 72 hours depending on the developmental cycle, infected cultures were sonicated, and the inoculum was used to perform a plaque assay, PCR and sequencing of PCR targets to identify putative recombinants (see below, Fig. S1).

The plaque assay was used to isolate clonally pure putative recombinants. The protocol was modified according to Somboonna *et al.* (20). Briefly, the first well of a 6-well plate with 60% confluent McCoy cell monolayers was infected with 100 to 500 µL of the co-infected shell vial from condition A, B or C, depending on the infection rate; seven serial 10-fold dilutions were used where the $2^{nd}$ and $7^{th}$ dilutions were applied to wells 1-6. After 24 h, 2 mL of agarose gel consisting of 0.5% agarose (Lonza, Rockland, ME) in phenol-red free MEM (Gibco), 10%



PeerJ Preprints | https://doi.org/10.7287/peerj.preprints.2489v1 | CC BY 4.0 Open Access | rec: 30 Sep 2016, publ: 30 Sep 2016

FBS and 1µg/ml Cycloheximide was added and topped with propagation medium with Gentamycin/Vancomycin or NGV-Amp B.

Following incubation for 4 to 16 hrs at 37 °C, 5% $CO_2$, the well with detectable but low-level infection was chosen to mark individual inclusions (no neighboring inclusions) at 200 x magnification. Individual inclusions were selected and picked using a sterile transfer pipet (Fisher Scientific) by punching a hole of 1-2 mm in diameter; the plug was transferred to a 1.5 mL Eppendorf vial (Hauppauge, NY) containing 500 µL propagation medium. The vial contents were sonicated once as described above and used to inoculate one shell vial per picked inclusion containing 500 µL propagation medium. Shell vials were centrifuged for 1 h as above and incubated for three days. Putative clones were passaged once into another similarly prepared shell vial. The infected material was collected for PCR and sequencing (see below), either by infection of a T25 flask (Greiner, North Carolina) and subsequent collection as described (21) or direct collection by sonication of the shell vials, centrifugation at 15,000 RPM for 5 min and aspiration of the supernatant. 100-500 µL of sonicated chlamydial suspension (depending on the infection rate) was used for a second passage into a shell vial as above. Once the infection of McCoy cells reached 100%, cultures were sonicated and frozen at -80°C.

**Identification of putative recombinants for genome sequencing.** DNA of the collected clones was extracted using the Roche High Pure PCR Product Purification Kit (Roche, Pleasanton, CA), and PCR was performed as previously described (20). All primers are listed in Table S1. Clones were considered putative recombinants if they had the following characteristics by PCR: Positive for the correct size band for the *tet*(C) gene; positive for the intergenic region (IGR) between the polymorphic membrane protein gene (*pmp*)B and *pmp*C using primers specific for



PeerJ Preprints | https://doi.org/10.7287/peerj.preprints.2489v1 | CC BY 4.0 Open Access | rec: 30 Sep 2016, publ: 30 Sep 2016

178 S45; negative for the *pmp*C region using primers specific for Rogers132; and positive for the
179 major outer membrane protein A gene (*omp*A) with confirmation of the S45 *ompA* genotype by
180 Sanger sequencing.

181 Putative clonal recombinants were then propagated in 0.063 µg/mL tetracycline (4x MIC
182 of S45) to grow stocks for whole-genome sequencing, MIC determination, and the *tet*(C)
183 stability assay (see below). After the first passage, a second plaque assay was performed as
184 above to ensure clonal purity. Picked clones were either grown as described above or directly
185 picked and inoculated into 100 µL HBSS (Gibco) prior to DNA extraction, PCR and *omp*A
186 sequencing.

187

188 **Genome sequencing.** Stocks of clonally purified putative recombinants were treated with DNase
189 prior to gDNA purification as described previously (21). Libraries for sequencing were prepared
190 from 0.5 to 1 µg of genomic DNA. Illumina MiSeq libraries were constructed using the Nextera
191 kit and sequenced using the 250 bp paired end protocol on a MiSeq instrument. The resulting
192 sequence data was assembled de novo using the SPAdes (22) software. The CONTIGuator web
193 service (23) was used to map assembled contigs against the Rogers132 strain. We visualized the
194 structure of the assemblies aligned against individual regions of the chromosome using the
195 Bandage graph visualization (24) software and its integrated BLAST tool. Querying of short
196 sequences against the raw sequence reads in FASTQ format was performed using the R
197 ShortRead (25) package.

198 The raw genome data generated for this study are deposited in the SRA database (the
199 accession no. is pending).

200



PeerJ Preprints | https://doi.org/10.7287/peerj.preprints.2489v1 | CC BY 4.0 Open Access | rec: 30 Sep 2016, publ: 30 Sep 2016

**Analysis of homologous recombination and *tet*(C)-containing cassette insertion into *C. suis* strain S45.** We used the parsnp rapid genome alignment tool, which is part of the Harvest suite (26) to identify regions of genome exchange in the recombinants. *De novo* assembled contigs of the recombinants were mapped against the S45 recipient genome reference and compared to the pattern of SNPs obtained when the Rogers132 donor was mapped against S45. Mosaic regions introduced by homologous recombination events appeared as clusters of 'Rogers132-like' SNPs in the background of the S45 genome. The approximate boundaries of recombination events were mapped as the edges of continuous runs of inserted SNPs.

**'SNP painting' to find regions of homologous recombination in mixed cultures.** We noted from preliminary analysis that recombinant DNA preparations in some cases also contained residual DNA from donor and/or recipient strains. To visualize the proportion of reads containing the donor and recipient backbone, we used a technique we called 'SNP painting'. We extracted two 25mer DNA sequences centered on each SNP identified between the donor and recipient reference sequences that had in their central position either the donor or recipient base. We challenged this reference SNP library against a 25mer database created from the FASTQ of the post-mating mixture using Jellyfish software (27). From the counts of the donor and recipient 25mers at each base, we were able to 1) map recombinant boundaries and 2) ascertain the extent of mixed populations using R software (28).

**Phylogenetic analysis.** Genes were aligned using PRANK (29). The R package Phangorn (30) was used to calculate maximum likelihood phylogeny using the Symmetric+GI model (chosen based on best fit). Trees were bootstrapped 100 times.



PeerJ Preprints | https://doi.org/10.7287/peerj.preprints.2489v1 | CC BY 4.0 Open Access | rec: 30 Sep 2016, publ: 30 Sep 2016

**MIC determination (tetracycline susceptibility *In vitro*) and *tet*(C) stability assay.** The MIC of all confirmed recombinants (by PCR and *ompA* genotyping) was tested directly from purified clones as described above for the parental strains. To test the stability of the recombinants regarding the presence of *tet*(C), recombinants were used to infect McCoy cell monolayers in shell vials at an MOI of 5. Cultures were passaged five times before they were challenged or not with tetracycline using three different conditions: A) no tetracycline; B) ½ $MIC_{TP}$ of the recombinant; and C) 4x MIC of the recombinant. Following challenge, we propagated each recombinant once under each condition and determined the MIC as described above. The recombinant without tetracycline was grown for another five passages (10 total) and was treated similarly as for passage five. The MIC was determined again after one additional passage. Additionally, DNA was extracted from samples of the recombinants obtained after every passage to confirm that the *omp*A genotype was identical to the recombinant prior to the start of the assay and to test for the presence of *tet*(C) using the PCR primers (Table 2).



PeerJ Preprints | https://doi.org/10.7287/peerj.preprints.2489v1 | CC BY 4.0 Open Access | rec: 30 Sep 2016, publ: 30 Sep 2016

## RESULTS

**Co-infection of S45 with the tetracycline resistant strains R19 and R27 does not yield recombinants.** Previous studies have shown that co-infection with R19 results in $tet^R$ *C. trachomatis* strains (17, 31). We aimed to obtain *tet*(C)-positive *C. suis* S45 recombinants by co-infecting S45 with three $tet^R$ *C. suis* strains representing the three *tet*(C)-containing cassette types: Cassette I (strain R19, complete cassette with all three segments); Cassette II (strain 27, without Segment 1: replication/mobilization protein genes); and Cassette III (strain Rogers132; without Segment 3: transposases) (Fig. 1). Eight co-infections with R19 were performed using various protocols, including the addition of R19 at 8 h or 24 h pi with S45, and pre-treatment of R19 with high doses of tetracycline prior to co-infection. However, the entire R19/S45 co-infection material tested negative for S45 by PCR using primers specific for the IGR of *pmpB/C* and by *ompA* genotyping (Table S1) immediately after tetracycline challenge (see Material and Methods). For one protocol, S45 was grown in shell vials prior to co-infection with R19 (MOI 0.5) at 9 h pi with S45 and challenged with only 0.25 µg/mL tetracycline. The initial infections were mixed and contained S45, but picked clones were either initially only positive for R19 by PCR using R19-specific primers for *pmpC* and by *omp*A genotyping or positive for R19 after two more passages (data not shown). R27 co-infection with S45 was attempted but no recombinants were identified.

***tet*(C)-containing cassette transfer to recipient strain under inhibitory and sub-inhibitory tetracycline concentrations.** Recombinants between Rogers132 and S45 were successfully generated by simultaneous co-infection or by infection with Rogers132 after S45 had been grown for 24 h (see Material and Methods). The success rate of acquiring recombinants was



PeerJ Preprints | https://doi.org/10.7287/peerj.preprints.2489v1 | CC BY 4.0 Open Access | rec: 30 Sep 2016, publ: 30 Sep 2016

equally low. We obtained seven putative recombinants (Rec2 to Rec8), which were propagated for whole-genome sequencing following a second plaque purification (Table 2). In subsequent genome analysis described below, several of the 'recombinants' turned out to be mixtures of strains or only recipients, but we use the original term to describe Rec2 to Rec8 in this manuscript. In detail, for Co-infection 1, 21 clones were Rogers132 (donor strain); 3 were S45 survivors (recipient strain) or mixed infections (including putative recombinant Rec 2); and 2 were true recombinants (Rec 3 and 4). For Co-infection 2, 11 were Rogers132; 18 were S45 or mixed infection (including putative recombinant Rec 6-8); and one was a true recombinant (Rec5). Rec2 and Rec8 were tetracycline sensitive after propagation while Rec6 was positive for both S45 and Rogers132 by *omp*A genotyping and for Rogers132 by *pmp*C PCR. Fig. 2 shows the PCR results for *tet*(C), *pmp*C and *pmp*B/C for each of the seven recombinants. Interestingly, we only obtained recombinants from co-infections performed in media containing sub-inhibitory (1/2 $MIC_{TP}$) or inhibitory (4 x MIC) concentrations of tetracycline for S45; no recombinants were obtained without tetracycline. Rec3, Rec4 and Rec5 were confirmed recombinants by genomic analyses (see below).

We evaluated whether the three confirmed recombinants of Rec3, Rec4 and Rec5 remained stable over the course of ten passages in the absence selective pressure, specifically without sub-inhibitory concentrations of tetracycline. After five passages, the recombinants were challenged or not (A) with low (B) and high (C) doses of tetracycline with subsequent analysis of their antibiotic susceptibility (see Materials and Methods). For each recombinant, every passage was collected and tested for the presence of *tet*(C). At the tenth passage, *omp*A genotyping was also performed to exclude the possibility of a small population of Rogers132 survivors. As expected, the confirmed Rec3, Rec4 and Rec5 recombinants remained PCR positive for *tet*(C)



PeerJ Preprints | https://doi.org/10.7287/peerj.preprints.2489v1 | CC BY 4.0 Open Access | rec: 30 Sep 2016, publ: 30 Sep 2016

throughout the course of the stability assay as did the *omp*A genotype (data not shown). In addition, all confirmed recombinants continued to be tetracycline resistant after Passages 5 and 10 with relatively high minimal inhibitory concentrations of 8-16 µg/mL (Table 3).

In contrast, tetracycline resistant putative recombinants Rec7 and Rec6 did not have any evidence of recombination. The former was *tet*(C) positive by PCR in the first five passages but negative in Passages 6 to 10 with an *omp*A sequence aligning to S45, indicating dominance of the sensitive parental strain, while the latter was *tet*(C) positive throughout the course of the assay and tetracycline resistant both at Passage 5 and 10 but aligned to Rogers132 (Table 3).

All recombinants (putative and confirmed) required growth in 0.064 µg/mL tetracycline (4x MIC S45) to produce stocks for genome sequencing. Attempts to propagate the clones in the absence of tetracycline often led to the loss of the *tet*(C) cassette (*tet*(C) PCR-negative). However, once stocks were produced, the confirmed recombinants remained stable throughout the ten passages performed in the absence of tetracycline for the stability assay.

**Frequency of recombination.** The frequency of potential recombinants, without selecting for mixed infection or Rogers132 survivors, was low. One co-infection experiment was performed for each of the two protocols under three different tetracycline conditions described in Material and Methods (see also Table 2). For protocol 1 (recipient-first co-infection), a total of 26 clones were picked with six clones per each tetracycline Condition: A (no tetracycline); B (1/2 $MIC_{TP}$ S45); and C (2x MIC S45). The co-infections for the three conditions were used to infect one 6-well plate per condition. Six to 11 clones were picked (26 total) per plate, resulting in two confirmed recombinants, Rec3 and Rec4, from Condition B. For protocol 2 (simultaneous co-infection), 30 clones were picked with ten clones each per Conditions A, B and C, resulting in



PeerJ Preprints | https://doi.org/10.7287/peerj.preprints.2489v1 | CC BY 4.0 Open Access | rec: 30 Sep 2016, publ: 30 Sep 2016

one confirmed recombinant, Rec5, originating from Condition B. Taken together, of the 56 clones, only seven (12.5%) were identified as putative recombinants, and three were confirmed (5.4%). For Condition B, the success rate was 15.0% (3/20).

**Heterogeneity of *tet*(C) cassette insertion into *C. suis* strain S45.** The seven putative recombinants described above were genome sequenced. We made a database of 4,864 SNPs between the Rogers donor and S45 recipient using parsnp (26) (Table S2) and used them as markers to distinguish potential recombination junctions in raw sequence data (Fig. 3). Aside from Rec6, which was a mixture of donor and recipient, the recombinants were predominantly comprised of the genetic backbone of S45, evincing our success in screening for the recipient following co-infection. Recombinant regions were determined at the approximate junctions between regions of 'S45-like' and 'Rogers-like' SNPs (Fig. 3a). While Rec 2 was PCR-positive for *tet*(C), there was undetectable recombination based on genome sequence analysis. Similarly, Rec7 had no evidence for recombinants. Rec3 and Rec4 were confirmed recombinants with identical *tet*(C) cassette insertion sites at Rogers132 coordinates of approximately 705,300 to 760,600 (the upstream and downstream cross-over regions varied in length because of sparse SNPs, affecting the ability to precisely determine coordinates – see below) in the S45 backbone. This region constitutes ~55,300 nucleotides (5.3% of the genome) including the *rrn* operons, consisting of the 16S, 23S and 5S rRNAs. The insertion spans from the Na(+)-translocating NADH-quinone reductase subunit F gene (*nqr*F) to the phosphoenolpyruvate carboxykinase [GTP] gene (*pck*G) in S45.

Rec5 was also a recombinant but with a much larger insertion containing the *tet*(C) cassette at Rogers132 coordinates of approximately 638,000 to 813,000 (Fig. 3a and 3b, right



PeerJ Preprints | https://doi.org/10.7287/peerj.preprints.2489v1 | CC BY 4.0 Open Access | rec: 30 Sep 2016, publ: 30 Sep 2016

plot), spanning the genomic region of Rogers132 2-dehydro-3-deoxyphosphooctonate aldolase gene (*kds*A) to the 3'(2'), 5'-bisphosphate nucleotidase gene (*cys*Q) in the S45 backbone. This region constitutes 175,000 nucleotides (16.6% of the genome). There were also second and third insertions within Rogers132 coordinates 529,000 to 538,000 in the S45 backbone (Fig. 3b, left plot), including the Rogers 132 putative general secretion pathway protein D gene (*gsp*D) to the secretion system effector C gene (*sse*C) family.

Although Rec6 was a mixture of donor and recipients, we identified a small recombinant region of ~40,000 nucleotides between the Rogers132 coordinates of ~856,780 to 884,340. These coordinates are in the *pmp*D and phenylalanine t-RNA ligase (*phe*S) genes (Fig. 3c). Rec8 had no evidence of any recombinants, consistent with the PCR results (Fig. 2), and was considered an S45 survivor.

Figure 4 shows the recombinant locations of the cassette and other insertion sites within the context of the entire circular genome for Rec3 and 4, and for Rec5. While the cassette was confirmed to reside within the invasion gene and within the two *rrn* operons for all 11 previously genome sequenced *C. suis* strains (15), the insertion in Rec3 and Rec4 included the *nqr*F gene extending to the *pck*G gene beyond the downstream *rrn* operon. The upstream crossover region is located within approximately 2.2kb, either in the gene *pck*G or its neighboring gene downstream encoding a hypothetical protein and in proximity to ribosomal bindings sites (RBS), whereas the downstream crossover region is found within *nqr*F (170 bp; Fig. 5A).

For Rec5, the cassette insertion encompassed the span from gene *cys*Q to *kds*A, which included the *rrn* operons and the *omp*A gene of Rogers132. The upstream crossover region is located within approximately 750 bp between the downstream end of the *kds*A gene or its neighboring genes tRNA-Arg (*tct*) and a hypothetical protein-encoding gene, while the



PeerJ Preprints | https://doi.org/10.7287/peerj.preprints.2489v1 | CC BY 4.0 Open Access | rec: 30 Sep 2016, publ: 30 Sep 2016

354 downstream crossover region is found in the *cys*Q gene, spanning 230 bp (Fig. 4, Fig. 5B). Both
355 crossovers are in proximity to RBSs, and palindromes are evident. In addition, we identified two
356 shorter recombinant regions located adjacent to each other between *kds*A and *pmp*BC (Fig. 4).
357 The larger of the two crossover sequences was found upstream within *gps*D (~380 bp) and
358 downstream, either in *mut*L or *ipg*C, spanning approximately 3kb (Fig. 6A), and in proximity to
359 RBSs with evidence for palindromes where one is at the site of the SNP at nucleotide position
360 2230 (Fig. 6, A.1.).The complete crossover region located within the *sse*C-like gene family was
361 found within the span of 1500 bp (Fig. 6B). Figure 6C shows a schematic of the two Rogers132
362 insertions.

363 In examining the plasmids for each recombinant, all except Rec7 had the S45
364 plasmid. Rec6 was a mixture of both S45 and Rogers132 plasmids. None of the plasmids
365 exhibited any genetic exchange.

366

367 **Heterogeneous structure of the *tet*(C)-containing cassette and phylogeny of *tet*(C) / *tet*R(C).**
368 As indicated previously (7, 15), the *tet*(C)-containing cassette can be divided into three segments
369 that are nearly identical for each strain though the order of the segments varies, resulting in three
370 distinct cassettes (Fig. 1). Segment 2 is the only segment present in all strains and contains *tet*(C)
371 as well as the tetracycline repressor gene [*tet*R(C)]. To better understand the phylogenetic
372 placement of these two genes, a BLASTN search was performed to identify related sequences in
373 other bacterial genera with identity coverage between 98% and 100%. Fig. 7 shows the
374 Maximum Likelihood (ML) phylogeny for *tet*(C). While there is strong support for two distinct
375 *C. suis* clades, there is insufficient resolution to determine the order in which the clades branched
376 off and not enough evidence to support multiple *tet*(C) acquisitions implied by the ML tree. In



PeerJ Preprints | https://doi.org/10.7287/peerj.preprints.2489v1 | CC BY 4.0 Open Access | rec: 30 Sep 2016, publ: 30 Sep 2016

377 contrast, *tet*R(C) is highly conserved across genera (Fig. S2). The *tet*(C) and *tet*R(C) genes are
378 preceded by a gene encoding hypothetical proteins both in *C. suis* and *A. salmonicida* but which
379 was annotated as part of the phage integrase family (*orf*E) on the plasmid pMC2 of an uncultured
380 bacterium isolated from swine manure with 98% identity cover [JN704639.1]. Additionally, that
381 plasmid further identified a mobile element IS101 upstream of *orf*E, which is also present on
382 Segment 2.



PeerJ Preprints | https://doi.org/10.7287/peerj.preprints.2489v1 | CC BY 4.0 Open Access | rec: 30 Sep 2016, publ: 30 Sep 2016

## DISCUSSION

Mutation, HGT, and genome rearrangement are the forces that shape the evolution of bacterial genomes (32). Most *Chlamydiaceae* genomes show evidence of intra-species recombination events (15, 18, 33–37) but little to no evidence for the presence of classic HGT acquired pathogenicity islands (38) or other foreign genes except for bacteriophage inserts in *Chlamydia pneumoniae* (39) and genes possibly acquired in the plasticity zone or invasin locus (40, 41). The most notable exception to this rule is *C. suis*, which is not only known for the possession of the *tet*(C)-containing cassette (7), but has also recently been reported to be highly recombinogenic compared to other *Chlamydia* species (15).

All three classes of *tet*(C)-containing cassettes described in the **11** $tet^R$ *C. suis* strain genomes sequenced to date (15, 42) were inserted at an identical site within the invasin gene (also referred to as the *ilp* or *inv*-like gene), which is flanked upstream by an *rrn* operon and downstream by *nqr*F (7, 15). It is likely that they all originated from one ancestral event, although other options are formally possible (15). The $tet^S$ strain S45 possesses an intact invasin gene as does *C. caviae* strain GPIC [AE015925.1], sharing 73% identity and 91% query cover by BLASTN search (40). No other *Chlamydia* species contain this gene. Similar to the *tet*(C) and *tet*R(C), we found that *ilp* is conserved within the *C. suis* species with the former two genes displaying high homology to European *C. suis* strains (Fig. S**3**) (43). These data suggest that the invasion gene is required for cassette insertion. However, Suchland et al. (17) demonstrated that *C. muridarum* strain MoPn and *C. trachomatis* strain $L_2$, both of which lack *ilp,* are able to acquire the *C. suis* strain R19 *tet*(C)-containing cassette *in vitro* by co-infection, while *C. caviae* was not receptive.



PeerJ Preprints | https://doi.org/10.7287/peerj.preprints.2489v1 | CC BY 4.0 Open Access | rec: 30 Sep 2016, publ: 30 Sep 2016

In a follow-up study, Jeffrey et al. (31) co-infected the *tet*(C)-positive and -negative $L_2$ recombinants from the former study with non-LGV *C. trachomatis* strains such as F and J to produce new tetracycline resistant recombinants. Neither study found specific nucleotide sequences that suggested a mechanism for *in vitro* recombination, although in the Suchland et al. study (17) the region including the cassette between the *rrn* operons of R19 was inserted into the downstream *rrn* operon of $L_2$ creating a recombinant. In addition to a similar localization of the cassette in the *rrn* operon, Jeffrey et al. (31) identified what appeared to be non-specific recombination (190 events in 12 recombinant strains) that occurred throughout the genome, unlike the R19/$L_2$ recombinants, suggesting that the progeny may have contained mixed infections despite selection of clones by limiting dilution.

In contrast to the successfully produced $tet^R$ *C. trachomatis* $L_2$ and *C. muridarum* recombinants with R19 (17), we were unable to produce any *tet*(C)-positive *C. suis* S45 recombinants after co-infection with R19 despite multiple attempts. Similarly, co-infections with R27 were unsuccessful because $tet^R$ strains outcompeted S45 within two to three passages. This observation was surprising, especially if we consider that resistance-determining accessory resistance genes are thought to generally impair rather than promote biological fitness of bacteria in the absence of antibiotics (44). One possible explanation for this is that S45 was isolated in the 1960s and adapted to cell culture in the laboratory, whereas the tetracycline resistant strain donors have only been cultured since the 1990s. To test this hypothesis, R19 or another strain with a similar cassette would have to be co-infected with a more recently isolated $tet^S$ *C. suis* strain in the absence of tetracycline.

Another noteworthy contrast to the previous co-infection studies is that we implemented three different tetracycline conditions. Suchland et al. (17) performed co-infections without any



PeerJ Preprints | https://doi.org/10.7287/peerj.preprints.2489v1 | CC BY 4.0 Open Access | rec: 30 Sep 2016, publ: 30 Sep 2016

antibiotics prior to challenge with a high dose of tetracycline. In addition to this, we included sub-inhibitory (0.004 µg/mL) and inhibitory concentrations (0.032 µg/mL) of tetracycline for S45. These conditions were based on the hypothesis that low concentrations of antibiotics promote the selection towards resistant bacteria (45). Indeed, all of the three confirmed recombinants (Rec3, Rec4, and Rec5) were originally grown in sub-inhibitory antibiotic concentrations, suggesting that mating is optimized by a multiplicity of donors. Only one putative recombinant was isolated from cultures that were not initially grown in tetracycline, which was later confirmed as an S45 survivor (Rec2). In order to confirm that sub-inhibitory concentrations of tetracycline promote the transfer of the *tet*(C) cassette, quantitative analysis is necessary. For example, three independent co-infection experiments with identical protocols could be performed with twenty to thirty clones picked per tetracycline condition instead of six to 10 as in our study. The number of recombinants could then compared among tetracycline conditions.

Dugan et al. (16) previously proposed that one or both transposases within IS*605* (termed ISc*s605* by Dugan et al.) were responsible for the integration of the genomic island into the *C. suis* chromosome. While the initial HGT event that brought the ancestral *tet*(C) cassette into *C. suis* probably involved transposition, we were able to demonstrate that transfer of the cassette between *C. suis* was through double crossover homologous recombination. Therefore, it is possible that homologous recombination between *C. suis* strains has been a significant factor in the recent spread of tetracycline resistance.

The recombination boundaries were not near the duplicated *rrn* operons as observed in the $tet^R$ *C. trachomatis* recombinants described by Suchland et al (17) and one of 12 sequenced recombinants in the study by Jeffrey et al (2013) but rather in conserved, syntenic genome



PeerJ Preprints | https://doi.org/10.7287/peerj.preprints.2489v1 | CC BY 4.0 Open Access | rec: 30 Sep 2016, publ: 30 Sep 2016

regions (Fig. 5; Fig. 6). In our previous study, comparative genomics was used to infer that putative ancestral recombination had occurred at high frequency across the *C. suis* genome (15). The recombination boundaries in Rec3 and Rec4 were identical, suggesting they arose from sibling plaques rather than independent events. The Rec3 and Rec4 boundaries overlapped genes that recognized recombinant regions, (CS00632 and CS00678) (15), but the large Rec5 recombination region did not (genes CS00570-572, CS00715). Furthermore, the small insertions of Rec5 were incorporated within one non-recombinant (CS00485) and two recombinant regions (CS00482, CS00488-489). It is unclear, with a limited number of *C. suis* genomes to compare to date, whether the observed patterns reflect selection, recombination hotspots or are purely stochastic. In inspecting the regions, inverted repeats, chi sites or direct target repeats that are typical permissive sites for recombination were not detected. However, the upstream crossover in Rec5 contained a tRNA (Fig. 5B). tRNAs are known to be acquired and involved in recombination for a diversity of bacteria (46, 47). Conserved regions such as RBSs, which were present within or near each cross-over region (Fig. 5 and 6), may also facilitate homologous recombination because gene function would not be altered, allowing new recombinants to be successful (48) as in the present study. It is notable that a similar lack of patterned recombination was noted in a recent study regarding beta-lactam and vancomycin resistance in *Enterococcus faecium*, in which the authors hypothesized that long sequences of highly homologous DNA were targets for recombination (49). Since the majority of *C. suis* strains isolated from farm animals are $tet^R$ (up to 89%) (50, 51) and *C. suis* shares 79.8% average nucleotide identity with *C. trachomatis*, the potential for homologous recombination and cassette transfer are high.

In summary, we present a co-infection model that produces recombinants, demonstrating for the first time that the *tet*(C)-containing cassette is transferred between *C. suis* strains by



PeerJ Preprints | https://doi.org/10.7287/peerj.preprints.2489v1 | CC BY 4.0 Open Access | rec: 30 Sep 2016, publ: 30 Sep 2016

474 homologous recombination without the need for Segment 3 transposases. We also discovered
475 that, while the frequency of recombination is low, sub-inhibitory concentrations of tetracycline
476 may promote transfer and that, rather than targeting highly polymorphic regions, recombination
477 occurs in long homologous sequences and genomic regions with tRNAs. Our model will serve as
478 a template for determining the mechanisms and frequency of cassette transfer among *Chlamydia*
479 species such as *C. trachomatis* that may co-infect humans with $tet^R$ *C. suis* zoonotic strains.
480 Cassette transfer would have major implications for public health approaches to treatment for
481 humans and domesticated animals alike.
482
483



PeerJ Preprints | https://doi.org/10.7287/peerj.preprints.2489v1 | CC BY 4.0 Open Access | rec: 30 Sep 2016, publ: 30 Sep 2016

## ACKNOWLEDGMENTS

We are indebted to Dr. Art Andersen for providing his collection of *Chlamydiaceae* species and strains for this research. This collection is now housed, maintained and curated in Dr. Dean's laboratory. We also thank Tyler Morgan for excellent technical assistance.

## FUNDING INFORMATION

This work was supported by Public Health Service grant from the National Institute of Health (R01 AI098843 to D.D. and T.D.R.); the National Science Foundation (NSF) (2009-65109-05760 to D.D.) and an Early Postdoctoral Mobility Fellowship grant from the Swiss National Science Foundation (SNSF) (P2ZHP3_158590 to H.M.).

## REFERENCE


1. **Davies J**, **Davies D**. 2010. Origins and evolution of antibiotic resistance. Microbiol Mol Biol Rev **74**:417–33.
2. **Andersson DI**, **Hughes D**. 2014. Microbiological effects of sublethal levels of antibiotics. Nat Rev Microbiol **12**:465–78.
3. **Liu YY**, **Wang Y**, **Walsh TR**, **Yi LX**, **Zhang R**, **Spencer J**, **Doi Y**, **Tian G**, **Dong B**, **Huang X**, **Yu LF**, **Gu D**, **Ren H**, **Chen X**, **Lv L**, **He D**, **Zhou H**, **Liang Z**, **Liu JH**, **Shen J**. 2016. Emergence of plasmid-mediated colistin resistance mechanism MCR-1 in animals and human beings in China: A microbiological and molecular biological study. Lancet Infect Dis **16**:161–168.
4. **Oppliger A**, **Moreillon P**, **Charrière N**, **Giddey M**, **Morisset D**, **Sakwinska O**. 2012. Antimicrobial resistance of Staphylococcus aureus strains acquired by pig farmers from pigs. Appl Environ Microbiol **78**:8010–8014.
5. **Blair JM**, **Webber MA**, **Baylay AJ**, **Ogbolu DO**, **Piddock LJV**. 2015. Molecular mechanisms of antibiotic resistance. Nat Rev Microbiol **13**:42–51.
6. **Capita R**, **Alonso-Calleja C**. 2013. Antibiotic-Resistant Bacteria: A Challenge for the Food Industry. Crit Rev Food Sci Nutr **53**:11–48.
7. **Dugan J**, **Rockey DD**, **Jones L**, **Andersen AA**. 2004. Tetracycline resistance in Chlamydia suis mediated by genomic islands inserted into the chlamydial inv-like gene. Antimicrob Agents Chemother **48**:3989–3995.
8. **Biswas S**, **Raoult D**, **Rolain J-M**. 2008. A bioinformatic approach to understanding antibiotic resistance in intracellular bacteria through whole genome analysis. Int J Antimicrob Agents **32**:207–220.




PeerJ Preprints | https://doi.org/10.7287/peerj.preprints.2489v1 | CC BY 4.0 Open Access | rec: 30 Sep 2016, publ: 30 Sep 2016

519 9. **Schautteet K**, **Vanrompay D**. 2011. Chlamydiaceae infections in pig. Vet Res **42**:29.

520 10. **Hoffmann K**, **Schott F**, **Donati M**, **Di Francesco A**, **Hässig M**, **Wanninger S**, **Sidler X**,
521 **Borel N**. 2015. Prevalence of chlamydial infections in fattening pigs and their influencing
522 factors. PLoS One **10**.

523 11. **Dean D**, **Rothschild J**, **Ruettger A**, **Kandel RP**, **Sachse K**. 2013. Zoonotic
524 Chlamydiaceae species associated with trachoma, Nepal. Emerg Infect Dis **19**:1948–1955.

525 12. **De Puysseleyr K**, **De Puysseleyr L**, **Dhondt H**, **Geens T**, **Braeckman L**, **Morré SA**,
526 **Cox E**, **Vanrompay D**. 2014. Evaluation of the presence and zoonotic transmission of
527 Chlamydia suis in a pig slaughterhouse. BMC Infect Dis **14**:560.

528 13. **De Puysseleyr L**, **De Puysseleyr K**, **Braeckman L**, **Morré SA**, **Cox E**, **Vanrompay D**.
529 2015. Assessment of Chlamydia suis Infection in Pig Farmers. Transbound Emerg Dis;
530 **doi: 10.1111/tbed.12446**

531 14. **Kohlhoff SA**, **Hammerschlag MR**. 2015. Treatment of Chlamydial infections: 2014
532 update. Expert Opin Pharmacother **16**:205–12.

533 15. **Joseph SJ**, **Marti H**, **Didelot X**, **Read TD**, **Deborah D**. 2016. Tetracycline selective
534 pressure and homologous recombination shape the evolution of Chlamydia suis: a recently
535 identified zoonotic pathogen. Genome Biol Evol.

536 16. **Dugan J**, **Andersen AA**, **Rockey DD**. 2007. Functional characterization of IScs605, an
537 insertion element carried by tetracycline-resistant Chlamydia suis. Microbiology **153**:71–
538 79.

539 17. **Suchland RJ**, **Sandoz KM**, **Jeffrey BM**, **Stamm WE**, **Rockey DD**. 2009. Horizontal
540 Transfer of Tetracycline Resistance among Chlamydia spp. in Vitro. Antimicrob Agents
541 Chemother **53**:4604–4611.



PeerJ Preprints | https://doi.org/10.7287/peerj.preprints.2489v1 | CC BY 4.0 Open Access | rec: 30 Sep 2016, publ: 30 Sep 2016

542 18. **Read TD**, **Joseph SJ**, **Didelot X**, **Liang B**, **Patel L**, **Dean D**. 2013. Comparative Analysis
543 of Chlamydia psittaci Genomes Reveals the Recent Emergence of a Pathogenic Lineage
544 with a Broad Host Range. MBio **4**:e00604–12–e00604–12.
545 19. **Suchland RJ**, **Geisler WM**, **Stamm WE**. 2003. Methodologies and cell lines used for
546 antimicrobial susceptibility testing of Chlamydia spp. Antimicrob Agents Chemother
547 **47**:636–642.
548 20. **Somboonna N**, **Mead S**, **Liu J**, **Dean D**. 2008. Discovering and differentiating new and
549 emerging clonal populations of Chlamydia trachomatis with a novel shotgun cell culture
550 harvest assay. Emerg Infect Dis **14**:445–453.
551 21. **Somboonna N**, **Wan R**, **Ojcius DM**, **Pettengill MA**, **Joseph SJ**, **Chang A**, **Hsu R**, **Read**
552 **TD**, **Dean D**. 2011. Hypervirulent Chlamydia trachomatis Clinical Strain Is a
553 Recombinant between Lymphogranuloma Venereum (L2) and D Lineages. MBio
554 **2**:e00045–11–e00045–11.
555 22. **Bankevich A**, **Nurk S**, **Antipov D**, **Gurevich A a.**, **Dvorkin M**, **Kulikov AS**, **Lesin VM**,
556 **Nikolenko SI**, **Pham S**, **Prjibelski AD**, **Pyshkin A V.**, **Sirotkin A V.**, **Vyahhi N**, **Tesler**
557 **G**, **Alekseyev M a.**, **Pevzner P a.** 2012. SPAdes: A New Genome Assembly Algorithm
558 and Its Applications to Single-Cell Sequencing. J Comput Biol **19**:455–477.
559 23. **Galardini M**, **Biondi EG**, **Bazzicalupo M**, **Mengoni A**. 2011. CONTIGuator: a bacterial
560 genomes finishing tool for structural insights on draft genomes. Source Code Biol Med
561 **6**:11.
562 24. **Wick RR**, **Schultz MB**, **Zobel J**, **Holt KE**. 2015. Bandage: Interactive visualization of de
563 novo genome assemblies. Bioinformatics **31**:3350–3352.
564 25. **Morgan M**, **Anders S**, **Lawrence M**, **Aboyoun P**, **Pagès H**, **Gentleman R**. 2009.



PeerJ Preprints | https://doi.org/10.7287/peerj.preprints.2489v1 | CC BY 4.0 Open Access | rec: 30 Sep 2016, publ: 30 Sep 2016

ShortRead: A bioconductor package for input, quality assessment and exploration of high-throughput sequence data. Bioinformatics **25**:2607–2608.

26. **Treangen TJ**, **Ondov BD**, **Koren S**, **Phillippy AM**. 2014. The Harvest suite for rapid core-genome alignment and visualization of thousands of intraspecific microbial genomes. Genome Biol **15**:524.

27. **Marçais G**, **Kingsford C**. 2011. A fast, lock-free approach for efficient parallel counting ofoccurrences of k-mers. Bioinformatics **27**:764–70.

28. **R Developement Core Team**. 2015. R: A Language and Environment for Statistical Computing. R Found Stat Comput **1**:409.

29. **Löytynoja A**. 2014. Phylogeny-aware alignment with PRANK. Methods Mol Biol **1079**:155–170.

30. **Schliep KP**. 2010. phangorn: Phylogenetic analysis in R. Bioinformatics **27**:592–593.

31. **Jeffrey BM**, **Suchland RJ**, **Eriksen SG**, **Sandoz KM**, **Rockey DD**. 2013. Genomic and phenotypic characterization of in vitro-generated Chlamydia trachomatis recombinants. BMC Microbiol **13**:142.

32. **Darmon E**, **Leach DRF**. 2014. Bacterial genome instability. Microbiol Mol Biol Rev **78**:1–39.

33. **Joseph SJ**, **Didelot X**, **Gandhi K**, **Dean D**, **Read TD**. 2011. Interplay of recombination and selection in the genomes of Chlamydia trachomatis. Biol Direct **6**:28.

34. **Joseph SJ**, **Read TD**. 2012. Genome-wide recombination in Chlamydia trachomatis. Nat Genet **44**:364–366.

35. **Joseph SJ**, **Didelot X**, **Rothschild J**, **de Vries HJC**, **Morre SA**, **Read TD**, **Dean D**. 2012. Population Genomics of Chlamydia trachomatis: Insights on Drift, Selection,



PeerJ Preprints | https://doi.org/10.7287/peerj.preprints.2489v1 | CC BY 4.0 Open Access | rec: 30 Sep 2016, publ: 30 Sep 2016

588 Recombination, and Population Structure. Mol Biol Evol **29**:3933–3946.

589 36. **Harris SR**, **Clarke IN**, **Seth-Smith HMB**, **Solomon AW**, **Cutcliffe LT**, **Marsh P**,
590 **Skilton RJ**, **Holland MJ**, **Mabey D**, **Peeling RW**, **Lewis DA**, **Spratt BG**, **Unemo M**,
591 **Persson K**, **Bjartling C**, **Brunham R**, **de Vries HJC**, **Morré SA**, **Speksnijder A**,
592 **Bébéar CM**, **Clerc M**, **de Barbeyrac B**, **Parkhill J**, **Thomson NR**. 2012. Whole-genome
593 analysis of diverse Chlamydia trachomatis strains identifies phylogenetic relationships
594 masked by current clinical typing. Nat Genet **44**:413–9, S1.

595 37. **Joseph SJ**, **Marti H**, **Didelot X**, **Castillo-Ramirez S**, **Read TD**, **Dean D**. 2015.
596 Chlamydiaceae genomics reveals interspecies admixture and the recent evolution of
597 Chlamydia abortus infecting lower mammalian species and humans. Genome Biol Evol
598 **7**:3070–3084.

599 38. **Nunes A**, **Gomes JP**. 2014. Evolution, phylogeny, and molecular epidemiology of
600 Chlamydia. Infect Genet Evol **23**:49–64.

601 39. **Rosenwald AG**, **Murray B**, **Toth T**, **Madupu R**, **Kyrillos A**, **Arora G**. 2014. Evidence
602 for horizontal gene transfer between Chlamydophila pneumoniae and Chlamydia phage.
603 Bacteriophage **4**:e965076.

604 40. **Liu Z**, **Rank R**, **Kaltenboeck B**, **Magnino S**, **Dean D**, **Burall L**, **Plaut RD**, **Read TD**,
605 **Myers G**, **Bavoil PM**. 2007. Genomic plasticity of the rrn-nqrF intergenic segment in the
606 Chlamydiaceae. J Bacteriol **189**:2128–2132.

607 41. **Read TD**, **Brunham RC**, **Shen C**, **Gill SR**, **Heidelberg JF**, **White O**, **Hickey EK**,
608 **Peterson J**, **Utterback T**, **Berry K**, **Bass S**, **Linher K**, **Weidman J**, **Khouri H**, **Craven**
609 **B**, **Bowman C**, **Dodson R**, **Gwinn M**, **Nelson W**, **DeBoy R**, **Kolonay J**, **McClarty G**,
610 **Salzberg SL**, **Eisen J**, **Fraser CM**. 2000. Genome sequences of Chlamydia trachomatis



PeerJ Preprints | https://doi.org/10.7287/peerj.preprints.2489v1 | CC BY 4.0 Open Access | rec: 30 Sep 2016, publ: 30 Sep 2016

MoPn and Chlamydia pneumoniae AR39. Nucleic Acids Res **28**:1397–406.

42. **Donati M**, **Huot-Creasy H**, **Humphrys M**, **Di Paolo M**, **Di Francesco A**, **Myers GSA**. 2014. Genome Sequence of Chlamydia suis MD56, Isolated from the Conjunctiva of a Weaned Piglet. Genome Announc **2(3)**:e00425–14.

43. **Donati M**, **Balboni A**, **Laroucau K**, **Aaziz R**, **Vorimore F**, **Borel N**, **Morandi F**, **Vecchio Nepita E**, **Di Francesco A**. 2016. Tetracycline Susceptibility in Chlamydia suis Pig Isolates. PLoS One **11**:e0149914.

44. **Andersson DI**, **Levin BR**. 1999. The biological cost of antibiotic resistance. Curr Opin Microbiol **2**:489–493.

45. **Cantón R**, **Morosini M-I**. 2011. Emergence and spread of antibiotic resistance following exposure to antibiotics. FEMS Microbiol Rev **35**:977–991.

46. **Bishop AL**, **Baker S**, **Jenks S**, **Fookes M**, **Gaora PO**, **Pickard D**, **Anjum M**, **Farrar J**, **Hien TT**, **Ivens A**, **Dougan G**. 2005. Analysis of the Hypervariable Region of the Salmonella enterica Genome Associated with tRNAleuX. J Bacteriol **187**:2469–2482.

47. **McDonald MJ**, **Chou C-H**, **Swamy KBS**, **Huang H-D**, **Leu J-Y**. 2015. The evolutionary dynamics of tRNA-gene copy number and codon-use in E. coli. BMC Evol Biol **15**:163.

48. **Gomes JP**, **Bruno WJ**, **Nunes A**, **Santos N**, **Florindo C**, **Borrego MJ**, **Dean D**. 2006. Evolution of Chlamydia trachomatis diversity occurs by widespread interstrain recombination involving hotspots. Genome Res **17**:50–60.

49. **García-Solache M**, **Lebreton F**, **McLaughlin RE**, **Whiteaker JD**, **Gilmore MS**, **Rice LB**. 2016. Homologous recombination within large chromosomal regions facilitates acquisition of beta-lactam and vancomycin resistance in Enterococcus faecium . Antimicrob Agents Chemother AAC.00488–16.



PeerJ Preprints | https://doi.org/10.7287/peerj.preprints.2489v1 | CC BY 4.0 Open Access | rec: 30 Sep 2016, publ: 30 Sep 2016

634 50. **Andersen A**, **Rogers D**. 1998. Resistance to tetracycline and sulphadiazine in swine C.
635 trachomatis isolates, p. 313–316. *In* Proceedings for the 9th international syposium on
636 human chlamydial infection.
637 51. **Di Francesco A**, **Donati M**, **Rossi M**, **Pignanelli S**, **Shurdhi A**, **Baldelli R**, **Cevenini R**.
638 2008. Tetracycline-resistant Chlamydia suis isolates in Italy. Vet Rec **163**:251–252.
639 52. **Kaltenboeck B**, **Kousoulas KG**, **Storz J**. 1993. Structures of and allelic diversity and
640 relationships among the major outer membrane protein (ompA) genes of the four
641 chlamydial species. J Bacteriol **175**:487–502.
642
643

644 **FIGURE LEGENDS**

645 **FIG. 1. The structure of the *tet*(C)-containing cassette is comprised of three unique**
646 **segments**. Shown is the *tet*(C)-containing cassette and its neighboring genes, depending on the
647 *C. suis* strain. The structure of the cassette comprises three diversely arranged segments (purple,
648 red and orange) consisting of different genes. Four cassette types, termed Class I to IV, have
649 been identified in ten *C. suis* strains: (I) contains all three segments in the listed segment order
650 (R19 and R24); (II) the cassette of Rogers132 is lacking segment 3, which contains transposases
651 IS200 and IS605; (III) the cassette of H5 is similar to that of cassette I but occurs in reverse
652 segment order; (IV) is missing segment 1 (replication/mobilization protein genes). *fts*K, DNA
653 translocase gene; *rrn* operon, consisting of 16S, 23S and 5S rRNA; *nqr*F, Na(+)-translocating
654 NADH-quinone reductase subunit F gene; *yaj*C, preprotein translocase subunit gene;
655 methyltrans., putative RNA methyltransferase gene; *rep*C, replication protein C gene; *rep*A,
656 replication protein A gene; H, hypothetical protein gene; T, Toxin *maz*F gene; relaxase, conjugal
657 transfer relaxase gene; CO, CO dehydrogenase maturation factor gene; ME, mobile element
658 IS101; *tet*C, tetracycline resistant gene class C; *tet*R, tetracycline repressor gene; tetracycline
659 resistance protein class A from transposon 1721; *tra.*, transposase (IS200); *put. trans.*, putative
660 transposase (IS605).

661

662 **FIG. 2. Strain-specific PCR primers identify putative recombinants**. Shown are the PCR
663 results of each putative recombinant Rec2 to Rec8. Rec6, a mixed population of S45 and
664 Rogers132, displays a faint positive band for Rogers132-specific *pmp*C (middle lane). All
665 putative recombinants were PCR positive for the S45-specific IGR between *pmp*B and *pmp*C
666 (top lane) and for *tet*(C).



PeerJ Preprints | https://doi.org/10.7287/peerj.preprints.2489v1 | CC BY 4.0 Open Access | rec: 30 Sep 2016, publ: 30 Sep 2016

667

668 **FIG. 3. Identification of Rogers132 insertion(s) and mixed infections in putative**
669 **recombinant genomes**. Plots recognizing recombinant regions were created by distinguishing
670 the two parental strains Rogers132 (red) and S45 (black) (see Materials and Methods). a)
671 Schematic of the putative recombinants Rec2, Rec3, Rec5, Rec6, Rec7 and Rec8 clockwise from
672 top left exemplifying crossover regions in Rec3 and Rec5; b) Enlarged region of the two
673 recombinant regions found in Rec5, and c) Schematic representation of recombinant regions
674 within Rec6, a putative recombinant, which was a mixed infection.

675

676 **FIG. 4. *Tet*(C)-cassette Insertions in the S45 Genome are Heterogeneous.** Shown is the site
677 of insertion for the three confirmed recombinants, Rec3/4 (top) and Rec5 (bottom), in the
678 circular S45 genome. PZ, plasticity zone; *cys*Q, adenosine-3'(2'),5'-bisphosphate nucleotidase;
679 rrn, rrn operon (16S rRNA, 23S rRNA, 5S rRNA); *nqr*F, Na(+)-translocating NADH-quinone
680 reductase subunit F; *pck*G, Phosphoenolpyruvate carboxykinase [GTP]; *omp*A, major outer
681 membrane protein A; *kds*A, 2-dehydro-3-deoxyphosphooctonate aldolase; *gsp*D, Putative general
682 secretion pathway protein D; hp, hypothetical protein.

683

684 **FIG. 5 Recombinant crossover regions in Rec3 and Rec4, and Rec5 based on sequence**
685 **alignments with S45 and Rogers132.** Shown are the nucleotide sequences of the crossovers up-
686 and downstream for Rec3 and Rec4 (A) and the large insertion of Rec5 (B). Numbers on top of
687 the sequences represent the positions relative to the respective gene. Gene IDs (e.g., CS00631)
688 refer to the annotation of Rogers132. Crossover regions are highlighted in grey with SNPs
689 indicated in magenta if the recombinants aligned to the S45 backbone and in green if they



PeerJ Preprints | https://doi.org/10.7287/peerj.preprints.2489v1 | CC BY 4.0 Open Access | rec: 30 Sep 2016, publ: 30 Sep 2016

690 aligned to Rogers132. Palindromes are indicated by blue letters, while tRNAs are highlighted in
691 light grey with white letters. The tRNA associated inverted repeats are highlighted in blue with
692 white letters. Putative ribosomal binding sites (RBS) are highlighted in red and further indicated
693 by "-RBS-" on top of the nucleotide sequence.
694
695 **FIG. 6 Recombinant crossover regions for Rec5 based on sequence alignments with S45**
696 **and Rogers132.** Shown are the nucleotide sequences of the small insertion of Rec5. A)
697 represents the slightly longer region upstream, while B) shows the shorter crossover region
698 downstream. Numbers on top of the sequences represent the positions relative to the respective
699 gene. Gene IDs (e.g., CS00631) refer to the annotation of Rogers132. Crossover regions are
700 highlighted in grey with SNPs indicated in magenta if the recombinants aligned to the S45
701 backbone and in green if they aligned to Rogers132. Blue letters indicate palindromes while
702 putative ribosomal binding sites (RBS) are highlighted in red and further indicated by "-RBS-"
703 on top of the nucleotide sequence.
704
705 **FIG. 7. *Tet*(C) reveals strong support for two clades.** Shown is the unrooted Baysian
706 phylogenetic tree of *tet*(C) for a number of tetracycline resistant bacteria (NCBI, BLASTN
707 search, identity cover: 98%) and ten *C. suis* strains, which correspond to two separate clades
708 (Clade 1: red; Clade 2: green) and H7 (blue).
709



PeerJ Preprints | https://doi.org/10.7287/peerj.preprints.2489v1 | CC BY 4.0 Open Access | rec: 30 Sep 2016, publ: 30 Sep 2016

## TABLES

**TABLE 1:** Characteristics of *C. suis* strains used in this study.

| Strains | Site/disease | Location | Isolation Date | MIC (µg/mL) | Cassette Class | Ref |
|---|---|---|---|---|---|---|
| S45 | Feces | Austria | 1960's | 0.016 | none | (52)[a] |
| Rogers132 | Intestine, lung, conjunctiva | Nebraska, USA | 1996 | 8 | II | (7)[a] |
| R19 | Enteritis | Nebraska, USA | 1992 | 16 | I | (7)[a] |
| R27 | Enteritis | Nebraska, USA | 1993 | 8 | IV | (7)[a] |

[a] Samples obtained from Dr. Art Andersen's collection (maintained and curated in Dr. Deborah Dean's lab)



PeerJ Preprints | https://doi.org/10.7287/peerj.preprints.2489v1 | CC BY 4.0 Open Access | rec: 30 Sep 2016, publ: 30 Sep 2016

715 **TABLE 2**. List of potential recombinants and their antibiotic susceptibility profiles**.**

| **Name** | **Parental Strains** | **Protocol 1 or 2** | **Tetracycline Condition A, B or C** | ***omp*A genotype / 132 *pmpC* PCR / S45 *pmpB/C* IGR PCR** | ***tet*(C) PCR** | **MIC (µg/mL)** |
|---|---|---|---|---|---|---|
| Rec2 | S45 / 132[a] | 1. 24 hpi, 2µg/mL | A. no tetracycline | S45 / - / S45 | positive | 0.125 |
| Rec3[b] | S45 / 132 | 1. 24 hpi, 2µg/mL | B. ½ $MIC_{Tp}$ S45 | S45 / - / S45 | positive | 8 |
| Rec4[b] | S45 / 132 | 1. 24 hpi, 2µg/mL | B. ½ $MIC_{Tp}$ S45 | S45 / - / S45 | positive | 8 |
| Rec5[b] | S45 / 132 | 2. Co-inf., 0.25 µg/mL | B. ½ $MIC_{Tp}$ S45 | 132 / - / S45 | positive | 4 |
| Rec6 | S45 / 132 | 2. Co-inf., 0.25 µg/mL | C. 2x MIC S45 | 132-S45 / 132 / - | positive | 8 |
| Rec7 | S45 / 132 | 2. Co-inf., 0.25 µg/mL | C. 2x MIC S45 | S45 / - / S45 | positive | 4 |
| Rec8 | S45 / 132 | 2. Co-inf., 0.25 µg/mL | C. 2x MIC S45 | S45 / - / S45 | negative | 0.064 |

716 [a]Rogers132**;** [b]true recombinant; (-), negative PCR

718 **TABLE 3**. Stability Assay for five recombinants, showing results for passage 5 (P5) and passage

719 10 (P10).

| Name | (*tet*[C] PCR) Start to P5 (A) | (*tet*[C] PCR) P5 (B / C) | (*tet*[C] PCR) P6 to P10 | MIC (µg/mL) P5 | MIC (µg/mL) P10 | *omp*A |
|---|---|---|---|---|---|---|
| Rec3 | + / + / + / + / + | + / + | + / + / + / + / + | 8 | 16 | S45 |
| Rec4 | + / + / + / + / + | + / + | + / + / + / + / + | 8 | 16 | S45 |
| Rec5 | + / + / + / + / + | + / + | + / + / + / + / + | 16 | 16 | 132[a] |
| Rec6 | + / + / + / + / + | + / + | + / + / + / + / + | 16 | 16 | 132[a] |
| Rec7 | + / + / + / + / + | + / - | - / - / - / - / - | 0.25 | ND | S45 |

720 [a] Denotes Rogers132

721 ND, Not done

722 **Supplementary Material**

723 **Figure S1. Co-infection Protocols and Conditions.** 1) Shown are the two co-infection
724 protocols, which consisted of a) staggered infection of the donor (strains R19, R27 and
725 Rogers132) 24 hours post infection with the recipient strain S45 (Protocol 1) and b) simultaneous
726 co-infection of recipient and donor after the recipient was first grown to 100% infection in shell
727 vials (Protocol 2). 2) Shown are the culturing conditions at the time of co-infection without
728 tetracycline (Condition A), subinhibitory concentrations of tetracycline (Condition B) and
729 inhibitory concentration of tetracycline (Condition C) for the recipient strain.

730

731 **Figure S2. The tetracycline repressor gene *tet*R(C) is highly conserved across genera.**
732 Shown is the unrooted Maximum Likelihood (ML) phylogenetic tree of *tet*R(C) for a number of
733 tetracycline resistant bacteria (NCBI, BLASTN search, identity cover: 98%) and ten *C. suis*
734 strains, which correspond to two separate clades (Clade 1: red; Clade 2: green) and H7 (blue).

735

736 **Figure S3. Phylogeny of invasin gene of *C. suis* and *C. caviae.*** Shown is the unrooted Baysian
737 phylogenetic tree of the chlamydial invasin gene that is found only in *C. suis* and *C. caviae*.

738

739 **Table S1:** Primers used to identify putative recombinants.

740

741 **Table S2**. Database of 4,864 SNPs identified between the Rogers132 donor and S45 recipient.

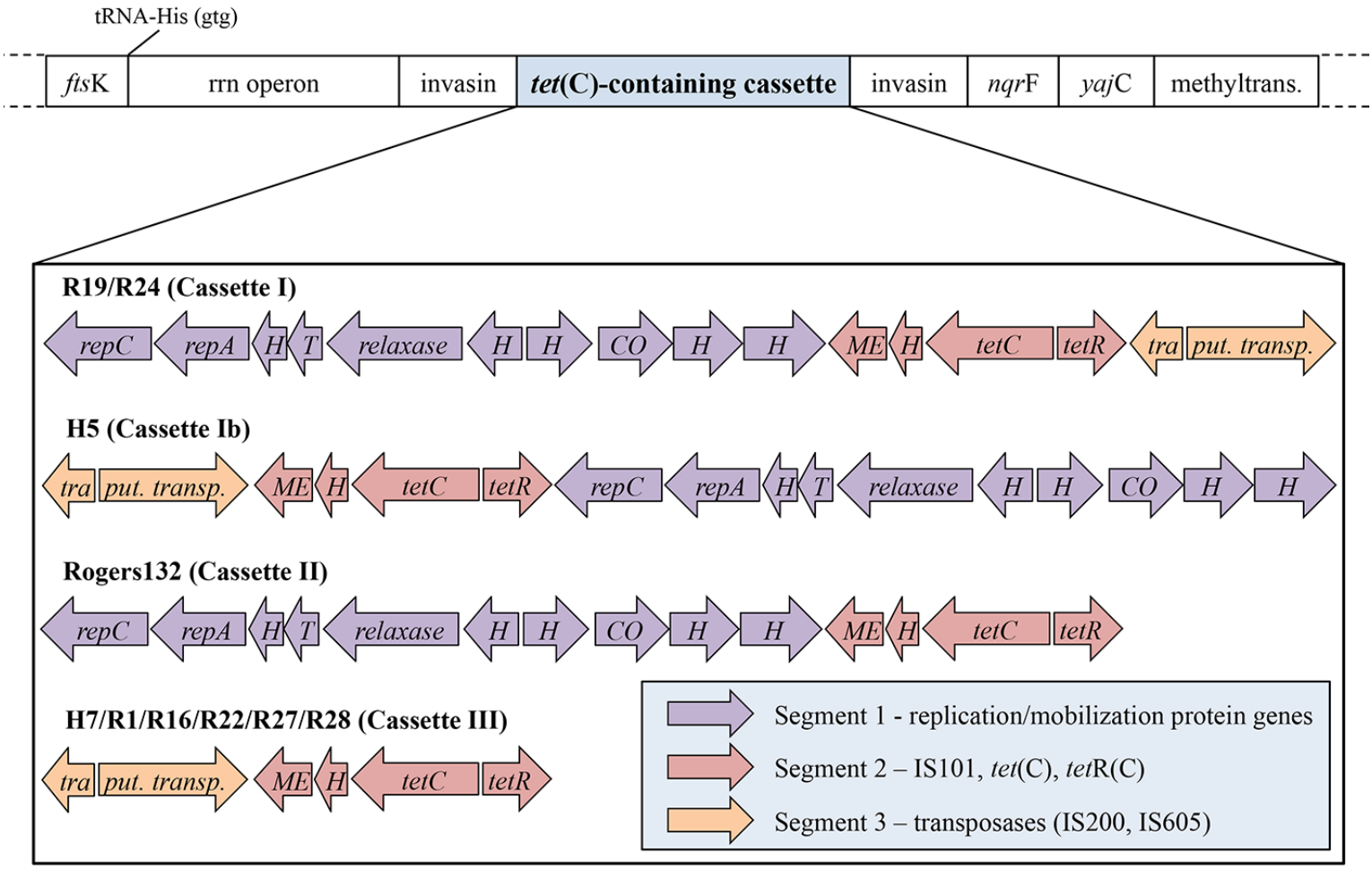


**FIG. 1. The structure of the *tet*(C)-containing cassette is comprised of three unique segments.** Shown is the *tet*(C)-containing cassette and its neighboring genes, depending on the *C. suis* strain. The structure of the cassette comprises three diversely arranged segments (purple, red and orange) consisting of different genes. Three cassette types have been identified in ten *C. suis* strains: (I) contains all three segments, though the cassette of H5 is arranged differently from R19 and R24; (II) the cassette of Rogers132 is lacking segment 3, which contains transposases IS200 and IS605; (III) is missing segment 1 (replication/mobilization protein genes). *fts*K, DNA translocase FtsK; rrn operon, 16S, 23S and 5S rRNA; *nqr*F, Na(+)-translocating NADH-quinone reductase subunit F; YajC, preprotein translocase subunit YajC; methyltrans., putative RNA methyltransferase; *rep*C, replication protein C; *rep*A, replication protein A; H, hypothetical protein; T, Toxin *Maz*F; relaxase, conjugal transfer relaxase; CO, CO dehydrogenase maturation factor; ME, mobile element IS101; *tet*C, tetracycline resistant gene class C; *tet*R, tetracycline repressor gene; (tetracycline resistance protein class A from transposon 1721); *tra.*, transposase (IS200); *put. trans.*, putative transposase (IS605).

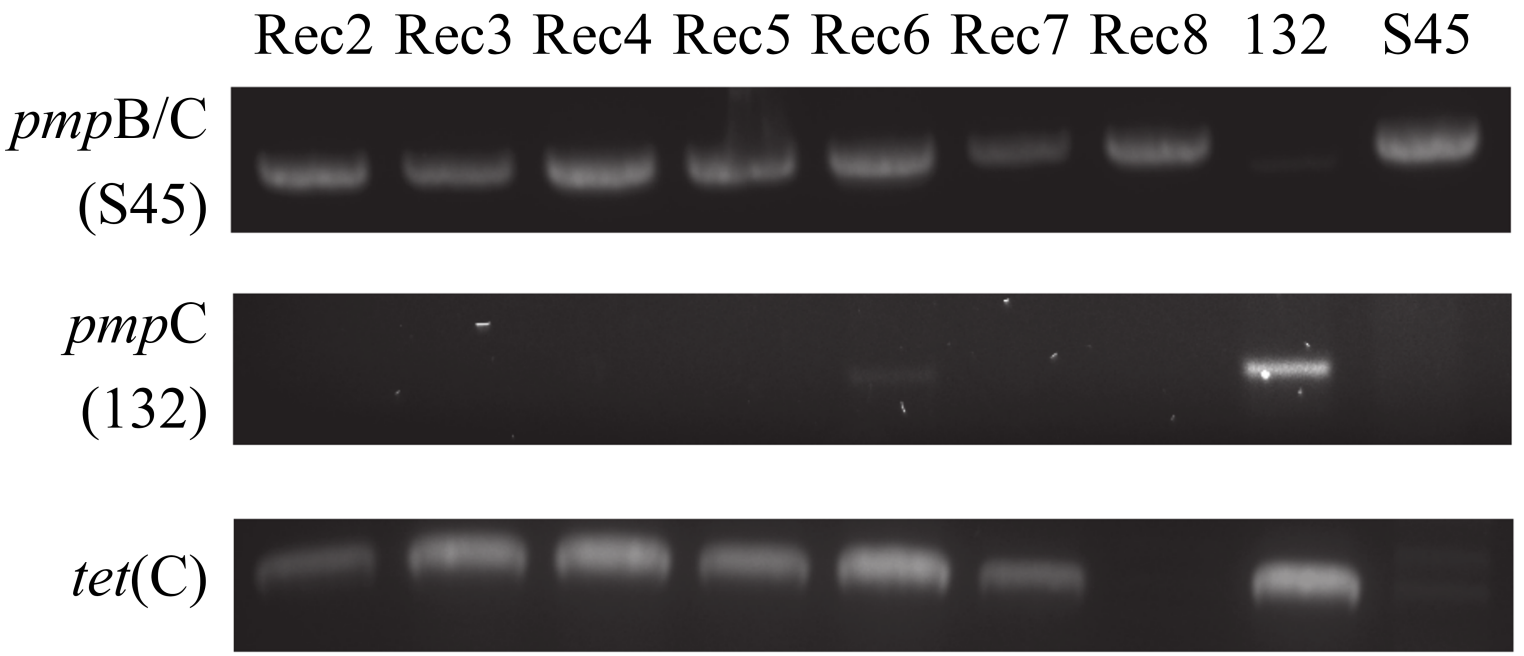


**FIG. 2. Strain-specific PCR primers identify putative recombinants**. Shown are the PCR results of each putative recombinant Rec2 to Rec8. Rec6, a mixed population of S45 and Rogers132, displays a faint positive band for Rogers132-specific *pmp*C (middle lane). All putative recombinants were PCR positive for the S45-specific IGR between *pmp*B and *pmp*C (top lane) and for *tet*(C).

PeerJ Preprints | https://doi.org/10.7287/peerj.preprints.2489v1 | CC BY 4.0 Open Access | rec: 30 Sep 2016, publ: 30 Sep 2016

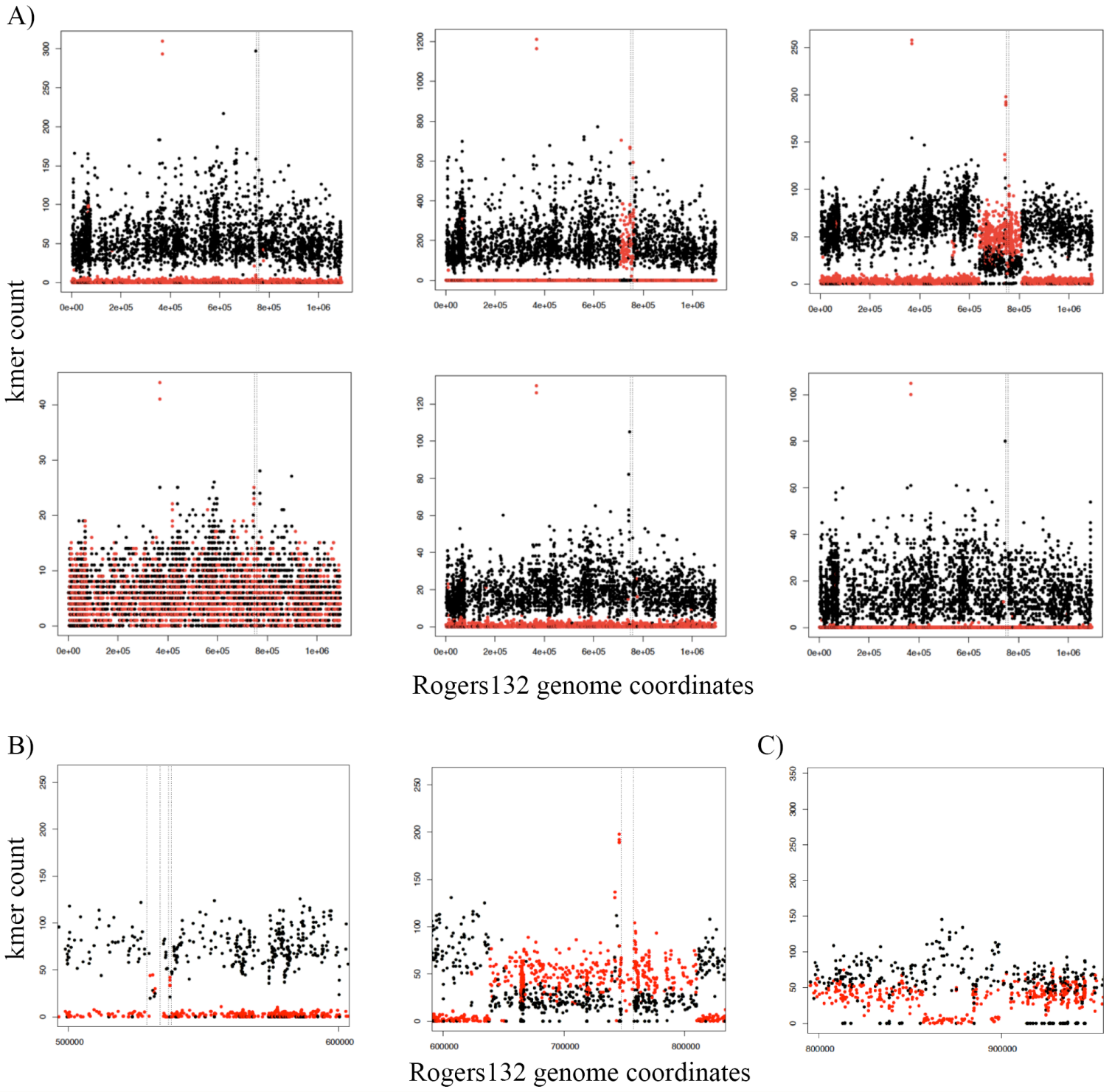


**FIG. 3. Identification of Rogers132 insertion(s) and mixed infections in putative recombinant genomes**. Plots recognizing recombinant regions were created by distinguishing the two parental strains Rogers132 (red) and S45 (black) (see Materials and Methods). a) Schematic of the putative recombinants Rec2, Rec3, Rec5, Rec6, Rec7 and Rec8 clockwise from top left exemplifying crossover regions in Rec3 and Rec5; b) Enlarged region of the two recombinant regions found in Rec5, and c) Schematic representation of recombinant regions within Rec6, a putative recombinant, which was a mixed infection.

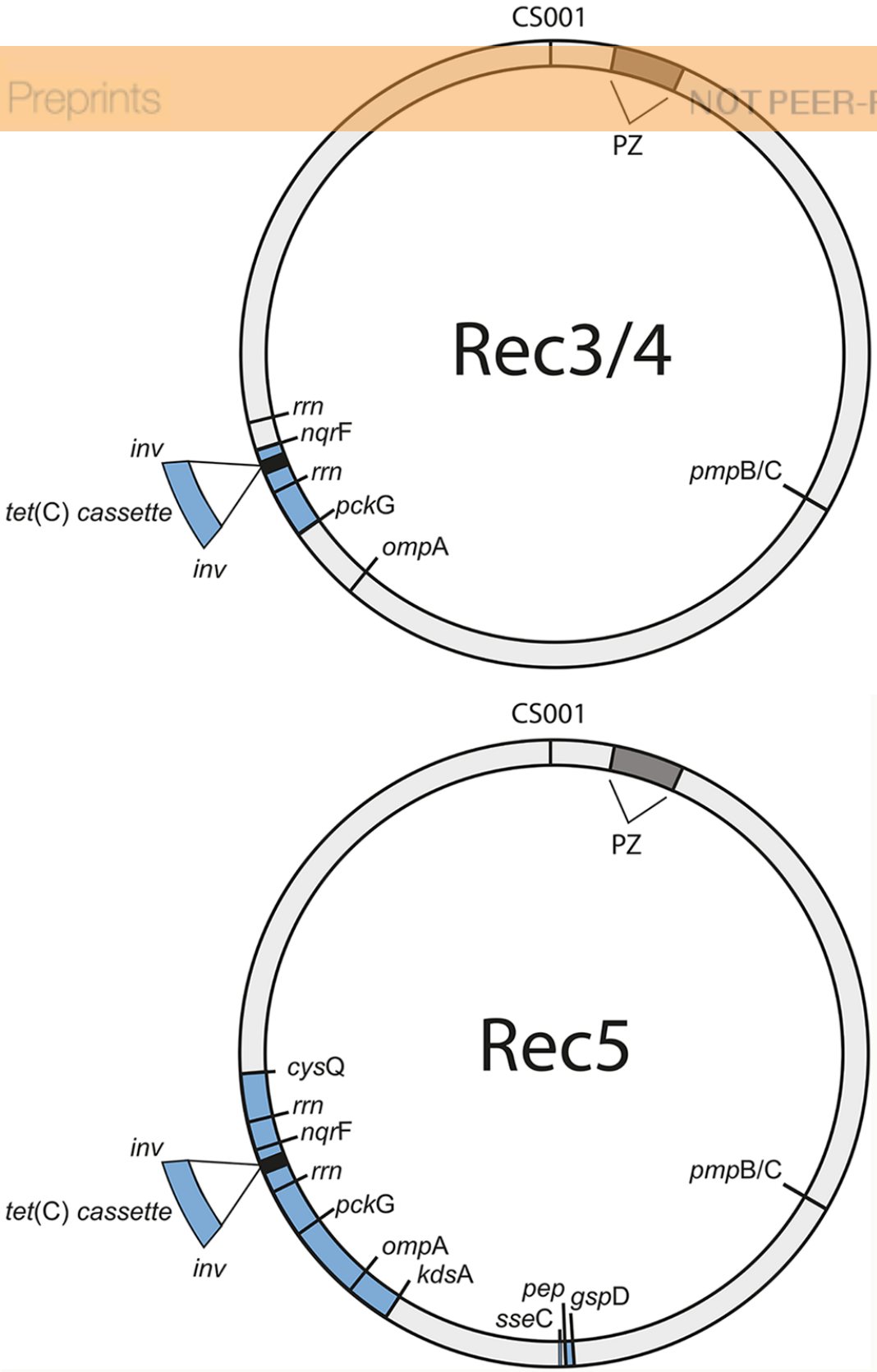


**FIG. 4. *Tet*(C)-cassette Insertions in the S45 Genome are Heterogeneous.** Shown is the site of insertion for the three confirmed recombinants, Rec3/4 (top) and Rec5 (bottom), in the circular S45 genome. PZ, plasticity zone; *cys*Q, adenosine-3'(2'), 5'-bisphosphate nucleotidase; rrn, rrn operon (16S rRNA, 23S rRNA, 5S rRNA); *nqr*F, Na(+)-translocating NADH-quinone reductase subunit F; *pck*G, Phosphoenolpyruvate carboxykinase [GTP]; *ompA*, major outer membrane protein A; *kds*A, 2-dehydro-3-deoxyphosphooctonate aldolase; *gsp*D, Putative general secretion pathway protein D; hp, hypothetical protein.

## A Insertion Rec3 and Rec4

**1. Upstream Crossover between phosphoenolpyruvate carboxykinase (*pckG*) to hypothetical protein gene (CS00631, CS00632)**

```
      pckG (631)  -RBS-                  166          180//hp (632) 370          -RBS-
132   GTCAGCAAATGCAGGAGTCCGGGGTCATGATCCCTGTAAATCCTGCGTTA//CCGAAAATGGCGGGATACAAGATCCTCTTCCCATAGAACAAGAAATCGTTGCTAAGTATCAAGCAGA
Rec3  GTCAGCAAATGCAGGAGTCTGGGGTCATGATCCCTTTAAATCCTGCGTTA//CCGAAAATGGCGGGATACAAGATCCTCTTCCCATAGAACAAGAAATCGTTGCTAAGTATCAAGCAGA
Rec4  GTCAGCAAATGCAGGAGTCTGGGGTCATGATCCCTTTAAATCCTGCGTTA//CCGAAAATGGCGGGATACAAGATCCTCTTCCCATAGAACAAGAAATCGTTGCTAAGTATCAAGCAGA
S45   GTCAGCAAATGCAGGAGTCTGGGGTCATGATCCCTTTAAATCCTGCGTTA//CCGAAAATGGCGGGATACAAGATCCTCTTCCCATAGAACAAGAACTCGTTGCTAAGTATCAAGCAGA

                                  470                                                -RBS-                                    549
132   ACTCAACACGCTACGTAATAAACTTAAACAGTCTGCGTTAACGGATGAGGAATATAAAAGGCTTTACGCGATTCCTCAAAACTTTGTGAAAGAGATAGAAAGCCTAAAGAAT
Rec3  ACTCAACACGCTACGTAATAAACTTAAACAGTCTGCGTTAACGGATGAGGAATATAAAAGGCTTTACGCGATTCCTCAAAACTTTGTGAAAGAGATAGAAAGCCTAAAGAAT
Rec4  ACTCAACACGCTACGTAATAAACTTAAACAGTCTGCGTTAACGGATGAGGAATATAAAAGGCTTTACGCGATTCCTCAAAACTTTGTGAAAGAGATAGAAAGCCTAAAGAAT
S45   ACTCAACACGCTACGTAATAAACTTAAACAGTTTGCGTTAACGGATGAGGAATATAAAAGGCTTTACGCGATTCCTCAAAACTTTGTGAAAGAGATAGAAAGCCTAAAGAAT
```

**2. Downstream Crossover in Na(+)-translocating NADH-quinone reductase subunit F (*nqrF*) (CS00678)**

```
      nqrF (678) 121                                        180
132   ATTGGGAAGCTTACTCAATTGGCCGAGTTCAAAAGCCTTGAACAAAAAGTTTGTTTTTTACGGGATCTTTACTATCCCAGCCTTTATCCAGATCTTCTTGTAAAGGCTGAGAGAGAACAAG
Rec3  ATTGGGAAGCTTACTCAATTGGCCGAGTTCAAAAGCCTTGAACAAAAAGTTTGTTTTTTACGGGATCTTTACTATCCCAGCCTTTATCCAGATCTTCTTGTAAAGGCTGAGAGAGAACAAG
Rec4  ATTGGGAAGCTTACTCAATTGGCCGAGTTCAAAAGCCTTGAACAAAAAGTTTGTTTTTTACGGGATCTTTACTATCCCAGCCTTTATCCAGATCTTCTTGTAAAGGCTGAGAGAGAACAAG
S45   ATTGGGAAGCTTACTCAATTGGCCGAGTTCAAAAGCCTTGAACAAAAAGTTTGTTTTTTATGGGATCTTTACTATCCCAGCCTTTATCCAGATCTTCTTGTAAAGGCTGAGAGAGAACAAG

                                                                                                                  349       360
132   GTGGTAGTGAAAGTTTGAAAATTCTTTTTCTAACCGTTCGTACTCTTCTTGGTAGATATTTTCCTTAAGAGAACGCGCGCCATACCACAACGTAAGCTCTCTGTTTGTTTGTTTATTTAG
Rec3  GTGGTAGTGAAAGTTTGAAAATTCTTTTTCTAACCGTTCGTACTCTTCTTGGTAGATATTTTCCTTAAGAGAACGCGCGCCATACCACAACGTAAGCTCTCTGTTTGTGTGTTTATTTAG
Rec4  GTGGTAGTGAAAGTTTGAAAATTCTTTTTCTAACCGTTCGTACTCTTCTTGGTAGATATTTTCCTTAAGAGAACGCGCGCCATACCACAACGTAAGCTCTCTGTTTGTGTGTTTATTTAG
S45   GTGGTAGTGAAAGTTTGAAAATTCTTTTTCTAACCGTTCGTACTCTTCTTGGTAGATATTTTCCTTAAGAGAACGCGCGCCATACCACAACGTAAGCTCTCTGTTTGTGTGTTTATTTAG
```

## B Insertion Rec5

**1. Upstream Crossover between 2-dehydro-3-deoxyphosphooctonate aldolase (*kds*A), tRNA-Arg (*tct*) and a hypothetical protein gene (CS00570, CS00571, CS00572)**

```
      kdsA (570) 763              790                 810/IGR kdsA/tct
132   AATCACACAAGGGCCTGCAATTAAAAGTAGTTTGTTGTCCGGGAACATAAAAGCGGTCCTTTTTTAGTTTAGAGAGAACTTTTGCTGTTAATCGAGTCTTTTAAAGACCTTATTGCTGAC
Rec5  AATCACACAAGGGCCTGCAATTAAAAGCAGTTTGTTGTCCGGGAACATAAAAGCGGTCCTTTTTTAGTTTAGAGAGAACTTTTGCTGTTAATCGAGTCTTTTAAAGACCTTATTGCTGAC
S45   AATCACACAAGGGCCTGCAATTAAAAGCAGTTTGTTGTCCGGGAACATAAAAGCGGTCCTTTTTTAGTTTAGAGAGAACTTTTGCTGTTAATCGAGTCTTTTAAAGACCTTATTGCTGAC

                                                    -RBS-
132   AGAAATTTGACTATACACCATTTATGTTTGATTGGTACGAGAAACCTTGAAAAATCCTCATGAAGATGGCTTTCTTGAAGAAAATAGAGGGATTCGGAGAGCGAAGGGTGGGAGATAAAC
Rec5  AGAAATTTGACTATACACCATTTATGTTTGATTGGTACGAGAAACCTTGAAAAATCCTCATGAAGATGGCTTTCTTGAAGAAAATAGAGGGATTCGGAGAGCGAAGGGTGGGAGATAAAC
S45   AGAAATTTGACTATACACCATTTATGTTTGATTGGTACGAGAAACCTTGAAAAATCCTCATGAAGATGGCTTTCTTGAAGAAAATAGAGGGATTCGGAGAGCGAAGGGTGGGAGATAAAC

                                                                                                                  tct (571) 1
132   AAATAGAGAAAGGAAGCTTAAAAGGAGAAGACGGAAGAGTGCTTCCAGAAAATCGATGTCTGCGGTATAGTATCTTCCATCTCTGCGAGGAGTTTTTTTGTTAGGGACCGATAGCTCAGT
Rec5  AAATAGAGAAAGGAAGCTTAAAAGGAGAAGACGGAAGAGTGCTTCCAGAAAATCGATGTCTGCGGTATAGTATCTTCCATCTCTGCGAGGAGTTTTTTTGTTAGGGACCGATAGCTCAGT
S45   AAATAGAGAAAGGAAGCTTAAAAGGAGAAGACGGAAGAGTGCTTCCAGAAAATCGATGTCTGCGGTATAGTATCTTCCATCTCTGCGAGGAGTTTTTTTGTTAGGGACCGATAGCTCAGT

132   GGATAGAGCATCCGCCTTCTAAGCGGATGGTCGCAGGTTCGAATCCTGCTCGGTCCAAGATTCCGCAGCTTCCTTTTTAGGTTTGGTTTCCTTTCTCTTGTGAAAAATCCTTTTGTCTCC
Rec5  GGATAGAGCATCCGCCTTCTAAGCGGATGGTCGCAGGTTCGAATCCTGCTCGGTCCAAGATTCCGCAGCTTCCTTTTTAGGTTTGGTTTCCTTTCTCTTGTGAAAAATCCTTTTGTCTCC
S45   GGATAGAGCATCCGCCTTCTAAGCGGATGGTCGCAGGTTCGAATCCTGCTCGGTCCAAGATTCCGCAGCTTCCTTTTTAGGTTTGGTTTCCTTTCTCTTGTGAAAAATCCTTTTGTCTCC

                  153 //hp (572) 218                                257                                293
132   AGTAAAATACAAAAAGAA//TTTTACCACGGTTCACAAAGAGATGGATCGTGCTCAGCGTGCTTCTAAGAAAATGCGTTCGGTCTATAAAGACTAA
Rec5  AGTAAAATACAAAAAGAA//TTTTACCACGGTTCACAAAGAGATGGATCGTGCTCAGCGTGCTTCTAAGAAAATGCGTTCGGTCTATAAAGACTAA
S45   AGTAAAATACAAAAAGAA//TTTTACCACGGTTCACAAAGAGATGGATCGTGCTCAGCGGGCTTCTAAGAAAATGCGTTCGGTCTATAAAGACTAA
```

**2. Downstream Crossover in adenosine-3'(2'),5'-bisphosphate nucleotidase (*cys*Q) (CS00715)**

```
      cysQ (715) 1                                523                                                                -RBS-
132   GAAAGGAAAAGAATGAGAGGGATTACAGATCATGAGCCCTTCTCGCCTTTCGCTGCTGAATAAATTTTAAAAGATCCATCTTTTGATGTAGGACAGGCAATGACAGAAAGAACAGGAGTGTG
Rec5  GAAAGGAAAAGAATGAGAGGGATTACAGATCATGAGCCCTTCACCTTTCGCTGCTGAATAAATTTTAAAAGATCCATCTTTTGATGTAGGACAGGCAATGACAGAAAGAACAGGAGTGTG
S45   GAAAGGAAAAGAATGAGAGGGATTACAGATCATGAGCCCTTCACCTTTCGCTGCTGAATAAATTTTAAAAGATCCATCTTTTGATGTAGGACAGGCAATGACAGAAAGAACAGGAGTGTG

132   TTCATAAAACAAAGAAAGAGCAACAGCAAAACAACGTTGTTTGATGAATCCTGAGGTGCCATCGATAGGATCTGTTAACCAAAATAGGGATGAGAGGGAGTTTTCTGGAGAGAGCGCGTG
Rec5  TTCATAAAACAAAGAAAGAGCAACAGCAAAACAACGTTGTTTGATGAATCCTGAGGTGCCATCGATAGGATCTGTTAACCAAAATAGGGATGAGAGGGAGTTTTCTGGAGAGAGCGCGTG
S45   TTCATAAAACAAAGAAAGAGCAACAGCAAAACAACGTTGTTTGATGAATCCTGAGGTGCCATCGATAGGATCTGTTAACCAAAATAGGGATGAGAGGGAGTTTTCTGGAGAGAGCGCGTG

                                  754                 780
132   ATAAAGATCTTGGGAAGAAACTTTCGGATCCAGCTGTTTGGCAAAGTGTATAATTTGAGG
Rec5  ATAAAGATCTTGGGAAGAAACTTTCGGATCCAGTTGTTTGGCAAAGTGTATAATTTGAGG
S45   ATAAAGATCTTGGGAAGAAACTTTCGGATCCAGTTGTTTGGCAAAGTGTATAATTTGAGG
```

**FIG. 5 Recombinant crossover regions in Rec3 and Rec4, and Rec5 based on sequence alignments with S45 and Rogers132.** Shown are the nucleotide sequences of the crossovers up- and downstream for Rec3 and Rec4 (A) and the large insertion of Rec5 (B). Numbers on top of the sequences represent the positions relative to the respective gene.. Gene IDs (e.g., CS00631) refer to the annotation of Rogers132. Crossover regions are highlighted in grey with SNPs indicated in magenta if the recombinants aligned to the S45 backbone and in green if they aligned to Rogers132. Palindromes are indicated by blue letters, while tRNAs are highlighted in light grey with white letters. The tRNA associated inverted repeats are highlighted in blue with white letters. Putative ribosomal binding sites (RBS) are highlighted in red and further indicated by "-RBS-" on top of the nucleotide sequence.

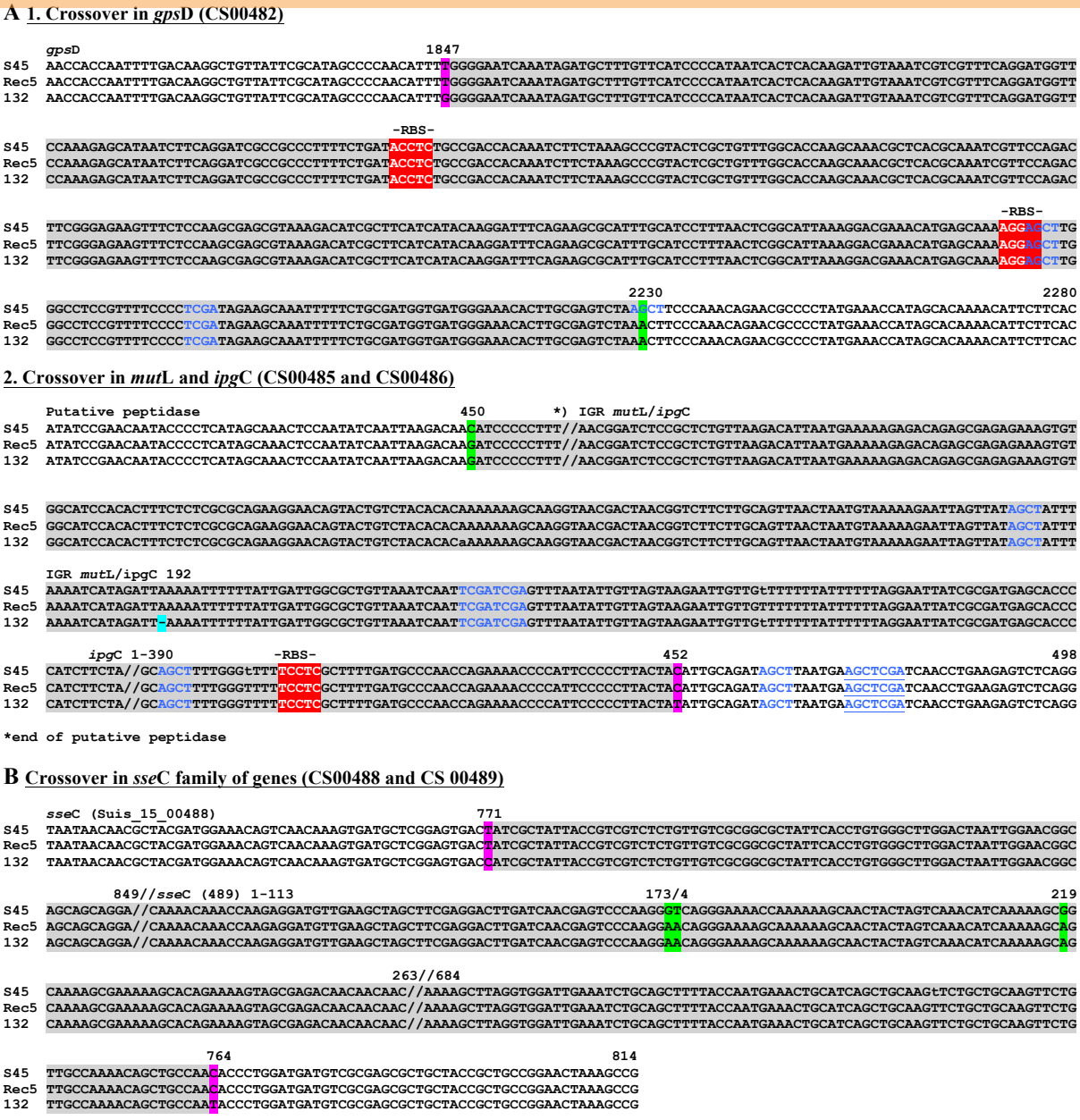


**FIG. 6 Recombinant crossover regions for Rec5 based on sequence alignments with S45 and Rogers132.** Shown are the nucleotide sequences of the small insertion of Rec5. A) represents the slightly longer region upstream, while B) shows the shorter crossover region downstream. Numbers on top of the sequences represent the positions relative to the respective gene. Gene IDs (e.g., CS00631) refer to the annotation of Rogers132. Crossover regions are highlighted in grey with SNPs indicated in magenta if the recombinants aligned to the S45 backbone and in green if they aligned to Rogers132. Blue letters indicate palindromes while putative ribosomal binding sites (RBS) are highlighted in red and further indicated by "-RBS-" on top of the nucleotide sequence.

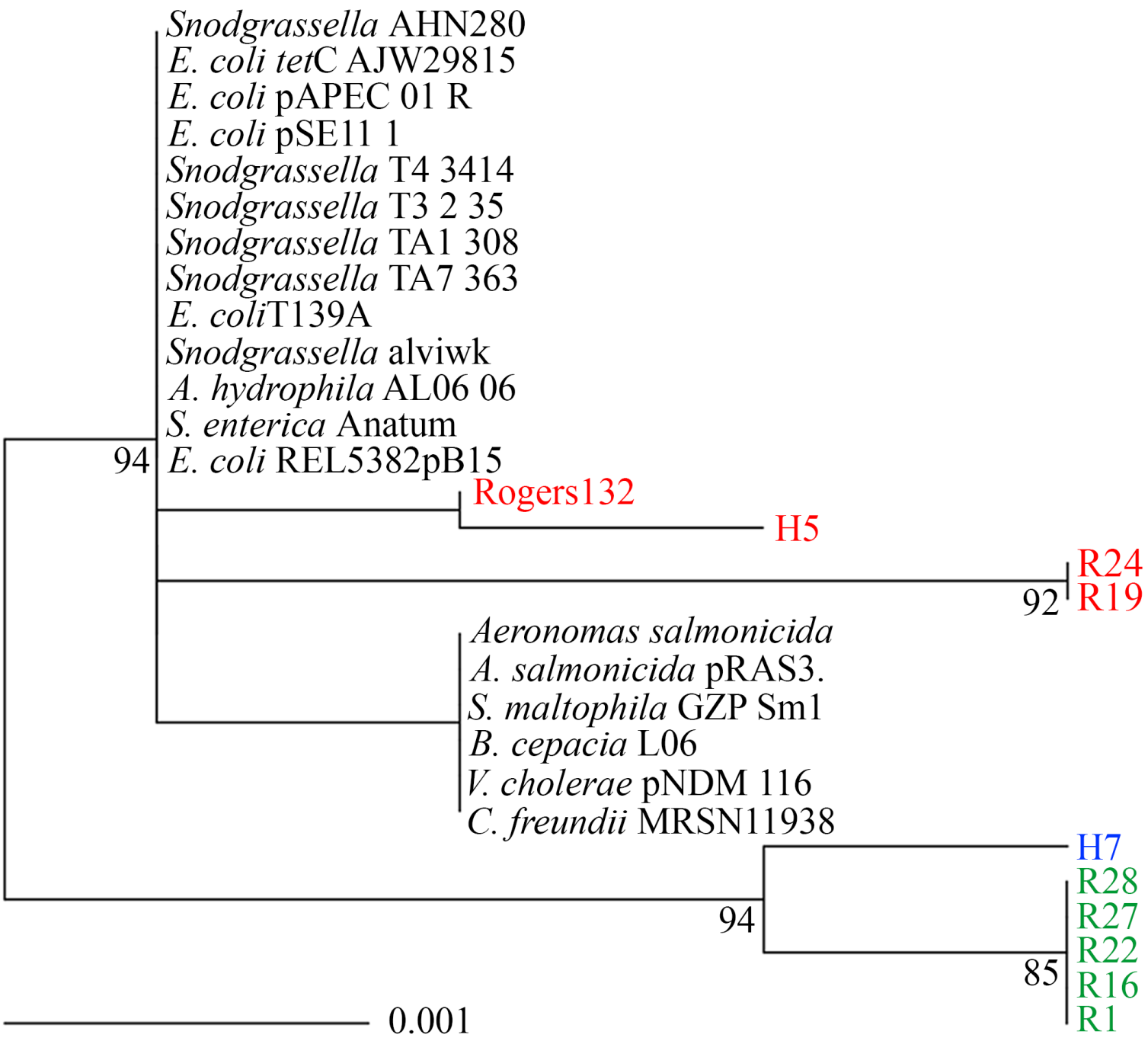


**FIG. 7. *Tet*(C) reveals strong support for two clades.** Shown is the unrooted Baysian phylogenetic tree of *tet*(C) for a number of tetracycline resistant bacteria (NCBI, BLASTN search, identity cover: 98%) and ten *C. suis* strains, which correspond to two separate clades (Clade 1: red; Clade 2: green) and H7 (blue).

PeerJ Preprints | https://doi.org/10.7287/peerj.preprints.2489v1 | CC BY 4.0 Open Access | rec: 30 Sep 2016, publ: 30 Sep 2016